SIAM J. Applied Dynamical Systems
Vol. 8, No. 4, pp. 1341–1381
© 2009 Society for Industrial and Applied Mathematics

Dynamical State and Parameter Estimation*

Henry D. I. Abarbanel†, Daniel R. Creveling‡, Reza Farsian‡, and Mark Kostuk‡

Abstract. We discuss the problem of determining unknown fixed parameters and unobserved state variables in nonlinear models of a dynamical system using observed time series data from that system. In dynamical terms this requires synchronization of the experimental data with time series output from a model. If the model and the experimental system are chaotic, the synchronization manifold, where the data time series is equal to the model time series, may be unstable. If this occurs, then small perturbations in parameters or state variables can lead to large excursions near the synchronization manifold and produce a very complex surface in any estimation metric for those quantities. Coupling the experimental information to the model dynamics can lead to a stabilization of this manifold by reducing a positive conditional Lyapunov exponent (CLE) to a negative value. An approach called dynamical parameter estimation (DPE) addresses these instabilities and regularizes them, allowing for smooth surfaces in the space of parameters and initial conditions. DPE acts as an observer in the control systems sense, and because the control is systematically removed through an optimization process, it acts as an estimator of the unknown model parameters for the desired physical model without external control. Examples are given from several systems including an electronic oscillator, a neuron model, and a very simple geophysical model. In networks and larger dynamical models one may encounter many positive CLEs, and we investigate a general approach for estimating fixed model parameters and unobserved system states in this situation.

Key words. data assimilation, synchronization manifold, conditional Lyapunov exponents, estimation in nonlinear systems, nonlinear prediction

AMS subject classifications. 49M30, 65K10, 65P40, 37M10

DOI. 10.1137/090749761

1. Introduction.

Estimating parameters and unobserved state variables in nonlinear dynamical systems is a matter of interest to many in control theory and nonlinear dynamics, as well as in various fields of physical and biological science and engineering [1, 2, 3, 4, 5, 6, 7, 8, 9, 10, 11, 12, 13, 14, 15, 16, 17, 18, 19, 20, 21, 22, 23, 24, 25, 26, 27]. In a common setting one has an experimental system described by a state vector $\mathbf{x}(t)$. We are interested in developing, on the basis of physical or biophysical principles, a model of this observed system. This model will have undetermined parameters that we wish to estimate from information in the observations.

*Received by the editors February 13, 2009; accepted for publication (in revised form) by T. Sauer July 9, 2009; published electronically October 14, 2009. This work was partially supported by the Office of Naval Research (ONR N00014-07-1-0741).

http://www.siam.org/journals/siads/8-4/74976.html

†Department of Physics, Marine Physical Laboratory (Scripps Institution of Oceanography), and Center for Theoretical Biological Physics, University of California, San Diego, La Jolla, CA 92093 (habarbanel@ucsd.edu). This author was partly supported by the ETH/University of Zurich, Institute for Neuroinformatics, during his sabbatical visit in January–April, 2009.

‡Department of Physics, University of California, San Diego, La Jolla, CA 92093-0402 (dcreveli@physics.ucsd.edu, rfarsian@ucsd.edu, mkostuk@physics.ucsd.edu). The fourth author was partly supported by the University of California through a San Diego Fellowship.

Copyright © by SIAM. Unauthorized reproduction of this article is prohibited.

Downloaded 11/01/17 to 161.45.254.242. Redistribution subject to SIAM license or copyright; see http://www.siam.org/journals/ojsa.php

Downloaded 11/01/17 to 161.45.254.242. Redistribution subject to SIAM license or copyright; see http://www.siam.org/journals/ojsa.php

Typically one can measure only a few components of the full state $\mathbf{x}(t)$ of the experimental system. Examples include a laser for which one can readily measure the magnitude of the electric field via the emitted light intensity but cannot directly measure the population inversion critical for lasing. In another arena, neurobiology, one can measure the time course of voltage changes across a cell membrane but cannot determine the percentage of Na^+ channels that are open as a function of time. When complex networks of systems such as these are constructed, dissecting the dynamics with only this partial observed information about the state of the network becomes an important challenge.

We will address the question of how one can use the measurement of a subset of the system dynamical variables to estimate unknown parameters in a physical or biological model of the system and also use the model to estimate the time dependence of the dynamical variables we do not observe. Once one has completed the model by estimating the parameters, the model can be used with new initial conditions and new external forcing or stimuli to make quantitative predictions of the future development of the full state of the system.

To use a model with dynamical variables $\mathbf{y}(t)$ to make a prediction or forecast from a set of observed data measured from some initial time t_I to a final time t_F, one must estimate any unknown fixed parameters in the model as well as all state variables at time t_F: $\mathbf{y}(t_F)$. Then model-based predictions or forecasts for $t > t_F$ can be accomplished. The methods we develop here will permit this, even for nonlinear systems with chaotic instabilities and for observations that include measurement noise [28]. We will explore the application of the methods to a variety of dynamical systems.

In this paper we introduce the general ideas involved in our procedures and explore several examples to illustrate how the methods work in practice.

To begin we will assume that we have measured only a single dynamical variable (think of light intensity or membrane voltage as above) out of the many giving the full state of the observed system $\mathbf{x}(t) = [x_1(t), x_2(t), x_3(t), \ldots]$. This measurement is a scalar projection of the full state, and we call it $P(\mathbf{x}(t))$. This measured quantity could be one of the components of the state vector, and for our discussion we will identify this projection as the first component of the state vector; namely, $P(\mathbf{x}(t)) = x_1(t)$. Also, we recognize that measurements are not made in continuous time but at discrete times $\{t_0, t_1, \ldots, t_{N-1}\}$ [29, 30, 31]. In many instances these times are spaced at regular intervals τ (the sampling time or the inverse of the sampling frequency in an experiment), so that $t_n = t_0 + n\tau$. We write, more or less interchangeably, without, we trust, confusion to the reader: $\mathbf{x}(t) = \mathbf{x}(t_n) = \mathbf{x}(n)$, $n = 0, 1, \ldots, N-1$.

We will describe how to use the information in the observations $x_1(n)$ to establish parameters and unobserved state variables using a model of the observed system.

2. Assimilating observed information into dynamical models.

2.1. Familiar least squares estimation. Using biophysical or physical reasoning based on properties of the experimental system, we construct a model of that system. This model contains L unknown parameters $\mathbf{p} = \{p_1, p_2, \ldots, p_L\}$. We write the collection of model dynamical variables as a D-dimensional vector $\mathbf{y}(n) = [y_1(n), \mathbf{y}_R(n)]$, where $y_1(n)$ corresponds to the observed $x_1(n)$, and the "rest" of the dynamical variables, $D-1$ of them, are indicated collectively by a subscript R.

We typically will not know the precise relationship between the dimension of $\mathbf{x}(n)$ and the

Copyright © by SIAM. Unauthorized reproduction of this article is prohibited.

Downloaded 11/01/17 to 161.45.254.242. Redistribution subject to SIAM license or copyright; see http://www.siam.org/journals/ojsa.php

D dimensions of $\mathbf{y}(n)$. As ever, we will use some sense of the embedding theorem [32, 33, 34] to select D large enough based on the data. If the dimension of the observed system is M, then $D = 2M + 1$ will be sufficient. As we know from studying long time series on strange attractors, a smaller dimension may well work in individual cases [35, 36].

Time is discretized in the observations, so we express the dynamics of the model system as the discrete time map $\mathbf{y}(n+1) = \mathbf{f}(\mathbf{y}(n), \mathbf{p})$:

$$\begin{aligned} y_1(t_{n+1}) &= y_1(n+1) = f_1(\mathbf{y}(n), \mathbf{p}) = f_1(\mathbf{y}(t_n), \mathbf{p}), \\ \mathbf{y}_R(t_{n+1}) &= \mathbf{y}_R(n+1) = \mathbf{f}_R(\mathbf{y}(n), \mathbf{p}) = \mathbf{f}_R(\mathbf{y}(t_n), \mathbf{p}), \end{aligned} \tag{1}$$

Maps relating the dynamical variables at time t_n to time t_{n+K} with $K > 1$ could also be used here. We remain with $K = 1$ in this paper. The discrete time dynamics could be an approximate solution format—Euler, Runge–Kutta, etc.—for the continuous time differential equations

$$\begin{aligned} \frac{dy_1(t)}{dt} &= F_1(\mathbf{y}(t), \mathbf{p}), \\ \frac{d\mathbf{y}_R(t)}{dt} &= \mathbf{F}_R(\mathbf{y}(t), \mathbf{p}). \end{aligned} \tag{2}$$

We wish to use the information in our observations $x_1(n)$ to estimate the parameters $\mathbf{p}$ and the unobserved states $\mathbf{y}_R(n)$. As a note of terminology, while natural scientists refer to the $\mathbf{y}$ dynamics as a model, within which one wishes to estimate parameters and use it for quantitative predictions, in control theory this is often denoted as an "observer." Observers are often constructed assuming knowledge of the fixed parameters in the model and are only required to estimate the unobserved states [2, 37, 38, 39, 40, 41, 42, 43, 44, 45, 46, 47].

One standard way to estimate the parameters $\mathbf{p}$ and the initial conditions for the model $\mathbf{y}_R(0)$ is to minimize the distance, in some metric, between the observations $x_1(n)$ and the model output $y_1(n)$. A familiar form for this is the least squares separation of these two quantities. We call this metric a cost function or an objective function, and we choose a least squares format for this:

$$C(\mathbf{y}(0), \mathbf{p}) = \frac{1}{2N} \sum_{n=0}^{N-1} \Big\{ (x_1(n) - y_1(n))^2 \Big\}. \tag{3}$$

We wish to minimize this quantity as our criterion for estimating the $\mathbf{p}$ and the $\mathbf{y}(0)$. There are many other metrics, of course, but if they compare the time series of the observations $x_1(n)$ with the equivalent time series output by the model $y_1(n)$ and seek to minimize the difference between them, they will need to face the same issues of instability we discuss now, and they will need regularization or stabilization similar to what we propose below.

From a dynamical systems point of view, minimizing the distance between the observations and the model output is a request that the synchronization submanifold $\mathbf{y}(n) \approx \mathbf{x}(n)$ of the combined "observed system plus model state space" ($\mathbf{x}$-space plus $\mathbf{y}$-space) be stable. This is needed so that we can successfully treat small variations about the state space in searching for $\mathbf{p}$ or $\mathbf{y}(0)$. As long as the model parameters are not identical to those in the observed system, we cannot mathematically expect identity synchronization $\mathbf{x}(n) = \mathbf{y}(n)$ but must rely

Copyright © by SIAM. Unauthorized reproduction of this article is prohibited.

Downloaded 11/01/17 to 161.45.254.242. Redistribution subject to SIAM license or copyright; see http://www.siam.org/journals/ojsa.php

on some form of generalized synchronization to hold. In analyzing experimental data this point is implicit but usually ignored.

An earlier analysis of an observer for chaotic systems [2] focused on the stability required in using the model to estimate unobserved states of the experimental system, assuming that the model system and its parameters were fully known. In this paper we are focused on examining models for complex systems, and we may not assume that the fixed parameters of the model are known in detail. In fact, we may not know that the model is even "right."

Indeed, our parameter and state estimation procedure is the tool we wish to use to estimate parameters, initial conditions, and unobserved states in order to establish properties of the model. The methods we introduce and explore here may be used to probe a set of proposed models as a tool for selection among them. The challenge in this is larger, then, than in establishing an "observer of chaos," where the model and the data source are assumed to obey precisely the same dynamics.

Stability of the synchronization manifold is required for minimization, as the surface in parameter space is fraught with local (and incorrect) minima when the observations and the model are chaotic unless the synchronization manifold is stable. In addition, we determine the parameters and initial conditions $\mathbf{y}(0)$ through a variational principle which uses the dynamical equations of a regularized (stabilized) model as constraints to be satisfied. Once we have estimated the parameters, we must remove the controls used for an observer or for stabilizing the synchronization manifold so that the model equations with estimated parameters are those suggested by the physical considerations that led to them and have no control terms remaining.

We now discuss the stability issues associated with minimizing the cost function equation (3). By minimizing this cost function we seek to estimate both the parameters $\mathbf{p}$ and the initial conditions $\mathbf{y}(0)$; the solutions to the discrete time or continuous time equations depend on both. We know $y_1(0) = x_1(0)$ from the observations.

We seek the cost function minimum by asking that

$$\frac{\partial C(\mathbf{y}(0),\mathbf{p})}{\partial p_k} = 0, \quad k = 1, 2, \ldots, L,$$
$$\frac{\partial C(\mathbf{y}(0),\mathbf{p})}{\partial y_a(0)} = 0, \quad a = 1, 2, \ldots, D; \tag{4}$$

however, these derivatives involve either

$$\frac{\partial y_1(n)}{\partial p_k} \quad \text{or} \quad \frac{\partial y_1(n)}{\partial y_a(0)}, \tag{5}$$

which, along with their counterparts

$$\frac{\partial y_R(n)}{\partial p_k} \quad \text{and} \quad \frac{\partial y_R(n)}{\partial y_a(0)}, \tag{6}$$

satisfy

$$\frac{\partial y_b(n+1)}{\partial p_k} = \sum_{c=1}^{D} Df_{bc}(\mathbf{y}(n),\mathbf{p}) \frac{\partial y_c(n)}{\partial p_k} + \frac{\partial f_b(\mathbf{y}(n),\mathbf{p})}{\partial p_k}, \tag{7}$$

$$\frac{\partial y_b(n+1)}{\partial y_a(0)} = \sum_{c=1}^{D} Df_{bc}(\mathbf{y}(n),\mathbf{p}) \frac{\partial y_c(n)}{\partial y_a(0)}. \tag{8}$$

Copyright © by SIAM. Unauthorized reproduction of this article is prohibited.

Downloaded 11/01/17 to 161.45.254.242. Redistribution subject to SIAM license or copyright; see http://www.siam.org/journals/ojsa.php

The $D \times D$ Jacobian matrix $\mathbf{Df}(\mathbf{y}, \mathbf{p})$ has components

$$Df_{ab}(\mathbf{y}, \mathbf{p}) = \frac{\partial f_a(\mathbf{y}, \mathbf{p})}{\partial y_b}, \tag{9}$$

which iterated along the orbit $\mathbf{y}(n)$ gives us

$$\frac{\partial y_b(n+1)}{\partial y_a(0)} = \left\{ \mathbf{Df}(\mathbf{y}(n)) \cdot \mathbf{Df}(y(n-1)) \cdot \cdots \mathbf{Df}(y(1)) \right\}_{ba}. \tag{10}$$

This can give rise to positive Lyapunov exponents and thus instability on the synchronization manifold. The instability will result in complicated surfaces in parameter $\mathbf{p}$ and initial condition $\mathbf{y}(0)$ space for $C(\mathbf{y}(0), \mathbf{p})$ with many local minima. As we show below, when we couple the observations to the model to accomplish regularization on the synchronization manifold, these Lyapunov exponents will become *conditional* Lyapunov exponents (CLEs) [35, 36, 48, 49], as the stability of the orbit $\mathbf{y}(n)$ is conditioned on its matching the observations $\mathbf{x}(n)$. It is the CLEs that we must focus on.

If one or more CLE is positive, the synchronization manifold is unstable, and the variations of orbits in the neighborhood of the synchronization manifold will be quite irregular. This would then lead the dependence of the cost function $C(\mathbf{y}(0), \mathbf{p})$ to be quite irregular in either the $\mathbf{p}$ or the $\mathbf{y}(0)$. This irregularity might be small for small times after a perturbation, but as the length of time of comparison of the data and the model increases, the data and the model orbits rapidly become incoherent with respect to each other. Indeed, the incoherence of the sum in the cost function should rise exponentially rapidly, as $\exp(n\tau\lambda)$ with λ the largest positive CLE, until it plateaus at some level where the distance between the observed and model time series is on the order of the variation in the time series itself.

We discuss first some examples with one positive CLE, and then we turn to a discussion of examples with more than one positive CLE.

2.2. Direct coupling of data to a model. The problem of irregular surfaces in parameter space has been recognized for some time [20, 23, 50, 51]. One way to eliminate these irregularities is to remove the positive CLE responsible for the instability of the synchronization manifold $\mathbf{x}(n) \approx \mathbf{y}(n)$. An approach to this is to add to the equation for $y_1(n)$ a coupling to the data that reduces the largest eigenvalue of the Jacobian matrix $Df_{ab}(\mathbf{y}(n), \mathbf{p})$ which, when transported around the orbit, produces CLEs in accordance with the Oseledec multiplicative ergodic theorem [52].

The following idea has been investigated in the dynamical systems literature for some years. Add a "control" term $k(x_1(n) - y_1(n))$ to the dynamics for $y_1(n)$ in order to synchronize the data $x_1(n)$ and the model

$$\begin{aligned} y_1(n+1) &= f_1(\mathbf{y}(n), \mathbf{p}) + k(x_1(n) - y_1(n)), \\ \mathbf{y}_R(n+1) &= \mathbf{f}_R(\mathbf{y}(n), \mathbf{p}), \end{aligned} \tag{11}$$

with a constant $k > 0$ that is "large enough," but, as we shall note, not "too large." This term takes $Df_{ab}(\mathbf{y}, \mathbf{p}) \to Df_{ab}(\mathbf{y}, \mathbf{p}) - \delta_{11}k$, and, when k is large enough, can reduce the positive CLE of the model plus control dynamics to negative values. With negative CLEs, the two solutions of the dynamics, $\mathbf{x}(n)$ and $\mathbf{y}(n)$, can synchronize.

Copyright © by SIAM. Unauthorized reproduction of this article is prohibited.

Downloaded 11/01/17 to 161.45.254.242. Redistribution subject to SIAM license or copyright; see http://www.siam.org/journals/ojsa.php

To establish what value of k is large enough for synchronization, we calculate

$$\frac{1}{2N}\sum_{n=0}^{N-1}\Big\{(x_1(n)-y_1(n))^2\Big\} \tag{12}$$

as a function of k. Here $x_1(n)$ and $y_1(n)$ are two solutions of the model with the same fixed parameters. The solution $x_1(n)$ has $k=0$, while $y_1(n)$ is evaluated with varying k as in (11). For $k \geq$ some k_s, the largest CLE becomes negative.

In effect we are asking whether the model can synchronize with itself when the dynamical variable equivalent to the data $x_1(t)$ is presented to it. If the model fails to synchronize under these circumstances, it will probably fail to synchronize with experimental data representing the same variable.

Once one has determined k_s, the cost function for $k > k_s$,

$$C(\mathbf{y}(0),\mathbf{p},k)=\frac{1}{2N}\sum_{n=0}^{N-1}\Big\{(x_1(n)-y_1(n))^2\Big\}, \tag{13}$$

can be used to determine the parameters $\mathbf{p}$ and initial conditions $\mathbf{y}(0)$, since the surfaces in the $\mathbf{p}$ and the $\mathbf{y}(0)$ should now be smooth as synchronization is stabilized. More precisely, since the synchronization manifold $\mathbf{x}(n)=\mathbf{y}(n)$ is stabilized, the search in parameter and initial condition space should not encounter the rough surfaces associated with instabilities as one moves around in $\mathbf{p}$ and $\mathbf{y}(0)$ space near those values, leading to synchronization. The k dependence in $C(\mathbf{y}(0),\mathbf{p},k)$ arises from the $y_1(n)$.

We illustrate these comments with data generated by the equations for a chaotic Colpitts oscillator [53], which we compare with output from the same model using a set of equations into which the data $x_1(t)$ is coupled, system (11). The Colpitts oscillator shown in Figure 1 is a familiar nonlinear oscillator constructed with standard linear R, L, C components and a single bipolar transistor. It has widespread technological applications, perhaps because of its simplicity and low cost.

From the circuit diagram, Figure 1, we can write the circuit equations,

$$\begin{aligned} C_2\frac{dV_E(t)}{dt} &= I_L(t)-I_0,\\ C_1\frac{dV_C(t)}{dt} &= I_L(t)+I_s(1-e^{-V_E(t)/V_T}),\\ L\frac{dI_L(t)}{dt} &= V_0-R_0I_L(t)-V_C(t)-V_E(t), \end{aligned} \tag{14}$$

with dynamical variables $V_E(t)$, the voltage at the transistor emitter; $V_C(t)$, the voltage at the transistor collector; and $I_L(t)$, the current through the inductor. We have assumed a particular form of the current-voltage curve for the transistor.

The fixed point of these equations in (V_E,V_C,I_L)-space can be moved to a convenient location through the scalings and translations

Copyright © by SIAM. Unauthorized reproduction of this article is prohibited.

Downloaded 11/01/17 to 161.45.254.242. Redistribution subject to SIAM license or copyright; see http://www.siam.org/journals/ojsa.php

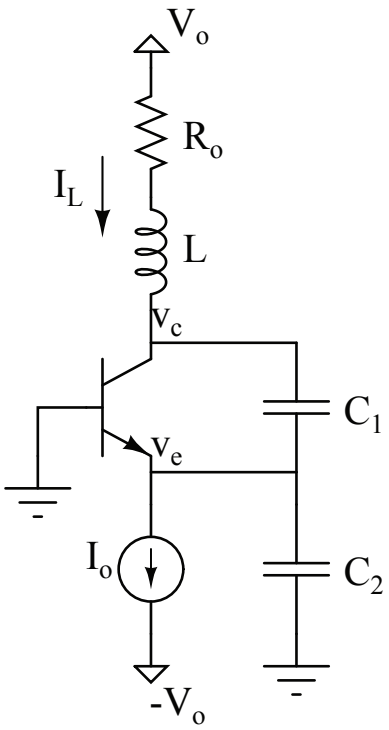

Figure 1. *Circuit diagram for the Colpitts oscillator.*

$$
\begin{aligned}
V_E(t) &= V_T x_1(t) + V_1, \\
I_L(t) &= I_0 x_2(t) + I_0, \\
V_C(t) &= V_T x_3(t) + V_2, \\
t &\to t\Delta t,
\end{aligned} \tag{15}
$$

where we have also defined dimensionless variables $\mathbf{x} = [x_1, x_2, x_3]$ and t. V_1 and V_2 are constants. The circuit equations now become

$$
\begin{aligned}
\frac{dx_1(t)}{dt} &= \alpha x_2(t), \\
\frac{dx_2(t)}{dt} &= \frac{(V_0 - R_0 I_0 - V_1 - V_2)\Delta t}{L I_0} - q x_2(t) - \gamma(x_1(t) + x_3(t)), \\
\frac{dx_3(t)}{dt} &= \eta\left(x_2(t) + 1 + \frac{I_s}{I_0} - \frac{I_s}{I_0} e^{-(x_1(t) + \frac{V_1}{V_T})}\right),
\end{aligned} \tag{16}
$$

with

$$
\begin{aligned}
\alpha &= \frac{I_0 \Delta t}{C_2 V_T}, \qquad & q &= \frac{R_0 \Delta t}{L}, \\
\gamma &= \frac{V_T \Delta t}{L I_0}, \qquad & \eta &= \frac{I_0 \Delta t}{C_1 V_T}.
\end{aligned} \tag{17}
$$

Copyright © by SIAM. Unauthorized reproduction of this article is prohibited.

Downloaded 11/01/17 to 161.45.254.242. Redistribution subject to SIAM license or copyright; see http://www.siam.org/journals/ojsa.php

In the transistor voltage-current relation, we note that $\frac{I_s}{I_0} \ll 1$, so we replace $1 + \frac{I_s}{I_0}$ by unity.

We will examine two different, but equivalent, forms of these equations. In the first form we place the fixed point at $\mathbf{x} = 0$ by choosing

$$\begin{aligned} e^{\frac{V_1}{V_T}} &= \frac{I_s}{I_0}, \\ V_2 &= V_0 - I_0 R_0 - V_1, \end{aligned} \tag{18}$$

giving us

$$\begin{aligned} \frac{dx_1(t)}{dt} &= \alpha x_2(t), \\ \frac{dx_2(t)}{dt} &= -\gamma(x_1(t) + x_3(t)) - q x_2(t), \\ \frac{dx_3(t)}{dt} &= \eta(x_2(t) + 1 - \exp(-x_1(t))). \end{aligned} \tag{19}$$

In this form α is a control parameter that, holding the other parameters fixed, leads to fixed point behavior of the oscillator when it is small. As α is increased, the oscillator expresses limit cycles; then, as it is increased further, to $\alpha \geq 3.5$ or so, chaotic orbits arise.

We will also examine the choice where we select $V_1 = 0$ and $V_2 = V_0 - I_0 R_0$, leading to the form

$$\begin{aligned} \frac{dx_1(t)}{dt} &= \alpha x_2(t), \\ \frac{dx_2(t)}{dt} &= -\gamma(x_1(t) + x_3(t)) - q x_2(t), \\ \frac{dx_3(t)}{dt} &= \eta(x_2(t) + 1 - \exp(-(x_1(t) + v_1))), \end{aligned} \tag{20}$$

writing $\frac{I_s}{I_0} = e^{-v_1}$.

We first use the form of (19). We solve these equations for $x_1(t_n) = x_1(n) = x_1(t_0 + n\tau)$ using some values of the parameters $\mathbf{p} = [\alpha, q, \gamma, \eta]$, and then compare the output of the same equations with the same parameters, with dynamical variables $\mathbf{y} = [y_1, y_2, y_3]$ plus a coupling term, namely,

$$\begin{aligned} \frac{dy_1(t)}{dt} &= \alpha y_2(t) + k(x_1(t) - y_1(t)), \\ \frac{dy_2(t)}{dt} &= -\gamma(y_1(t) + y_3(t)) - q y_2(t), \\ \frac{dy_3(t)}{dt} &= \eta(y_2(t) + 1 - \exp(-y_1(t))), \end{aligned} \tag{21}$$

by forming the cost function

$$C(\mathbf{p}, \mathbf{y}(0), k) = \frac{1}{2N} \sum_{n=0}^{N-1} \Big\{ (x_1(n) - y_1(n))^2 \Big\} \tag{22}$$

Copyright © by SIAM. Unauthorized reproduction of this article is prohibited.

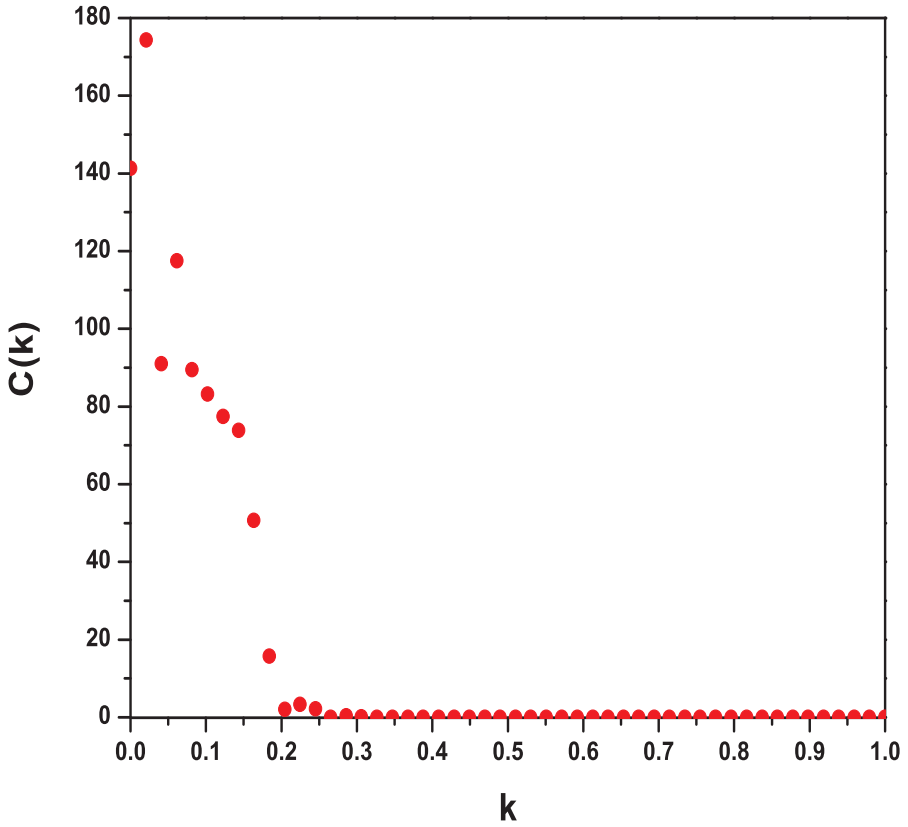

Figure 2. *The synchronization error between two identical coupled Colpitts oscillators as a function of the fixed coupling strength k. These oscillators are synchronized for $k \geq 0.25$.*

and examining the dependence on k. The dependence on k comes from $y_1(n)$. We selected the parameter values $\alpha = 5.0$, $\gamma = 0.0797$, $q = 0.6898$, and $\eta = 6.2723$, where the orbits in three-dimensional space are chaotic.

We first ask when the Colpitts oscillator synchronizes with itself, and in Figure 2 we see that this synchronization occurs at $k_s \approx 0.25$. Above this value for k the $C(\mathbf{p}, \mathbf{y}(0), k)$ goes to zero, indicating synchronization.

To examine the effect of synchronization (or the effect of its absence) on our ability to determine the parameters in the equations generating the data stream $x_1(t)$, we now evaluate the dependence of the cost function on k and on one of the parameters, here η, while the other three parameters are held at the values noted above. We evaluate

$$C(\eta) = \frac{1}{2N} \sum_{n=0}^{N-1} \left\{ (x_1(n) - y_1(n))^2 \right\} \tag{23}$$

as a function of η for various values of the coupling k. The dependence on η comes from $y_1(n)$. In Figure 3 we show $C(\eta)$.

For the two values of k smaller than $k_s \approx 0.25$, namely $k = 0.0$ and $k = 0.045$, we see that the instability of the synchronization manifold manifests itself as significant interference

Copyright © by SIAM. Unauthorized reproduction of this article is prohibited.

Downloaded 11/01/17 to 161.45.254.242. Redistribution subject to SIAM license or copyright; see http://www.siam.org/journals/ojsa.php

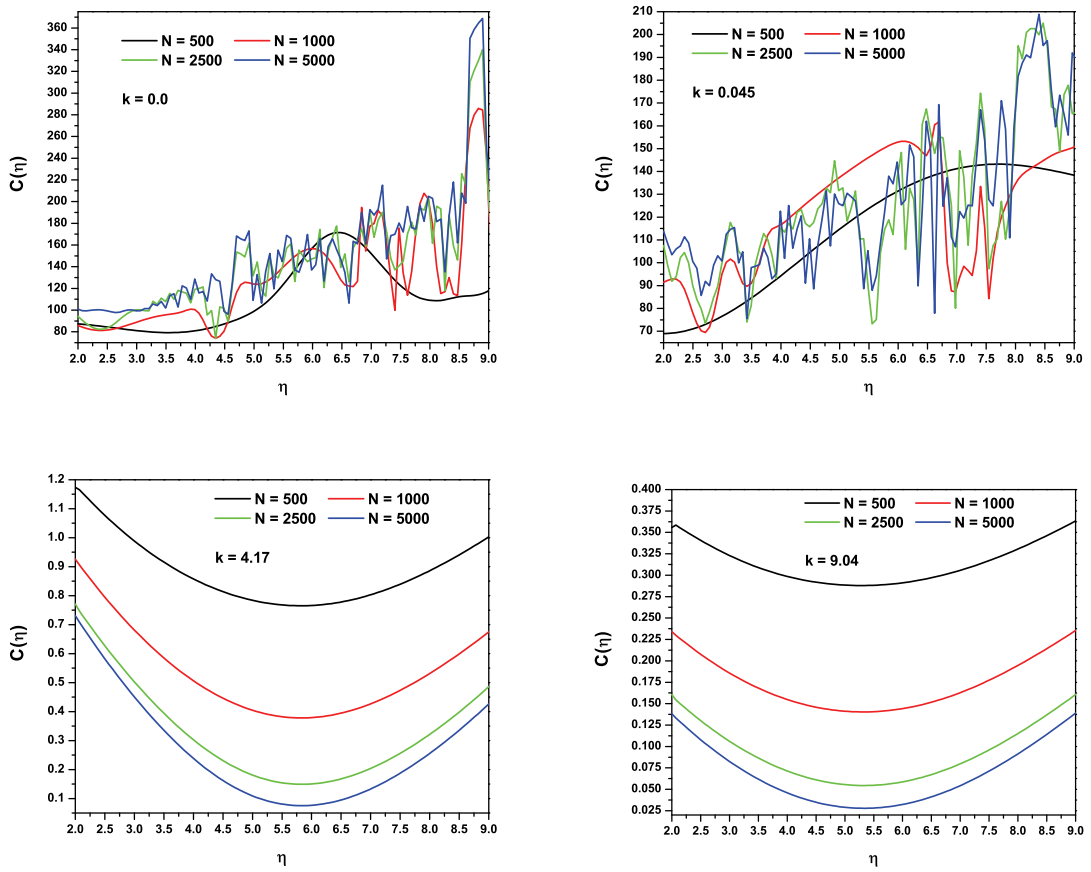

Figure 3. *Two Colpitts oscillators with state variables given by* $\mathbf{x}(t) = [x_1(t), x_2(t), x_3(t)]$ *and* $\mathbf{y}(t) = [y_1(t), y_2(t), y_3(t)]$ *are coupled with a term* $k(x_1(t) - y_1(t))$. *The least squares error (cost) function* $C(\eta)$ *is plotted for various* k. *The minimum of* $C(\eta)$ *should determine* η; *the value in the input data is* $\eta_{model} = 6.2723$. *Upper-left panel: For* $k = 0$ *the cost function develops complex multiple local minima that interfere with the determination of* η. *This structure comes from the positive CLE of the* $\mathbf{y}$ *system, that is, the instability of the synchronization manifold. Upper-right panel: At* $k = 0.045$ *synchronization has not occurred, and the surface in* η *is still quite ragged. Bottom-left panel: At* $k = 4.17$ *the oscillators are chaotic and synchronized. The surface in* η *becomes smooth, and the value of* $C(\eta)$ *decreases. Bottom-right panel: At* $k = 9.04$ *the surface in* η *remains smooth, and the value of* $C(\eta)$ *decreases.*

or mutual incoherence of the two signals $x_1(n)$ and $y_1(n)$. When k is larger than the synchronization threshold, we see that the surfaces in the parameter η become smooth and the cost function decreases significantly. Note the changing vertical scales for the various panels in Figure 3.

This figure also illustrates the following: the irregular shape of the η dependence and the appearance of multiple local minima arise when we increase the number of terms in the sum over time, forming the cost function. This is as it should be because the instability on the synchronization manifold grows as $e^{\lambda n \tau}$ with $\lambda > 0$, and this needs some time $n\tau \geq \lambda^{-1}$ to manifest itself and make the model (observer) results $y_1(n)$ decorrelate from the "data" $x_1(n)$.

Copyright © by SIAM. Unauthorized reproduction of this article is prohibited.

Downloaded 11/01/17 to 161.45.254.242. Redistribution subject to SIAM license or copyright; see http://www.siam.org/journals/ojsa.php

Downloaded 11/01/17 to 161.45.254.242. Redistribution subject to SIAM license or copyright; see http://www.siam.org/journals/ojsa.php

The use of a constant k to couple the information from $x_1(n)$ to the dynamics for $y_1(n)$ is known as a Luenberger observer (LO) after its exploration, originally in linear systems, around 1970 by Luenberger [40, 41, 42, 43]. As an "observer," its purpose was to allow the model (known as the "observer"), with fixed parameters the same as the source of the data $x_1(n)$, to learn from the model equations and the transmitted signal $x_1(n)$ about the other, unobserved, state variables $\mathbf{y}_R(n)$. When k is too small, one cannot estimate the parameters, and the states are badly determined as well.

There are some important issues we need to address with this observer formulation when used with respect to parameter and state estimation. If k is very large, the term $k(x_1(n) - y_1(n))$ dominates the dynamics for any vector field $f_1(\mathbf{y}, \mathbf{p})$ and makes parameter estimation numerically very difficult, if not impossible. When $k(x_1(n) - y_1(n))$ dominates the vector field $f_1(\mathbf{y}, \mathbf{p})$, then synchronization of the data and the model variable $y_1(n)$ occurs regardless of the model.

One can also see this in the lower panels of Figure 3, as $|x_1(n) - y_1(n)|$ should be approximately k^{-1} to contribute to the dynamics. This leads the cost function to decrease as k^{-2}. This means finding the zero of the cost function derivatives becomes increasingly difficult as k is large. Indeed, in the limit of $k \to \infty$, we would simply replace the state variable $y_1(n)$ in the model/observer with the data $x_1(n)$, and we arrive at the Pecora–Carroll [48] synchronization strategy, studying $\mathbf{y}_R(n+1) = \mathbf{f}_R(x_1(n), \mathbf{y}_R(n), \mathbf{p})$. While there is no theoretical limit to the size of the coupling term at the beginning of the estimation procedure, in practice numerical difficulties may begin to emerge when the product of the data timestep τ and the coupling k is greater than unity.

Most importantly, if k is fixed and not too large during the estimation procedure, this may, indeed, allow the model to act as an observer of the unobserved states $\mathbf{x}_R(n)$. However, when the procedure is completed, we are left with a different dynamical system, by the term $k(x_1(n) - y_1(n))$, than the one we developed from physical reasoning. A preferred situation would be to have this term $k(x_1(n) - y_1(n))$ absent at the end of our estimation procedure, leaving us the desired physical model

$$\begin{aligned} y_1(n+1) &= f_1(\mathbf{y}(n), \mathbf{p}), \\ \mathbf{y}_R(n+1) &= \mathbf{f}_R(\mathbf{y}(n), \mathbf{p}), \end{aligned} \tag{24}$$

with accurately estimated fixed parameters $\mathbf{p}$. If we accomplish the accurate estimation of the $\mathbf{p}$ with $k \to 0$, this allows the prediction of trajectories from new initial conditions and with, if needed, new external forcing, and has no reference to the observer or coupling to a previous set of data as embodied in a nonzero term $k(x_1(n) - y_1(n))$.

The role of the coupling or control k is to smooth out the parameter surface in the cost function, allowing us to move near the minimum of the cost function that we seek. Once we have reached the neighborhood of the minimum with the assistance of the regularization from the control, we should be able to reach that minimum as we systematically remove or turn off k, thus ensuring that the estimated parameter set corresponds to our original physically motivated model.

2.3. Oseledec's theorem. In the context of the LO or the dynamical system with constant coupling of the data into a model, we can make a statement using Oseledec's theorem about

Copyright © by SIAM. Unauthorized reproduction of this article is prohibited.

Downloaded 11/01/17 to 161.45.254.242. Redistribution subject to SIAM license or copyright; see http://www.siam.org/journals/ojsa.php

the conditions under which the approach will succeed. The same general statement will apply when we discuss cases with more than one positive CLE below. We proceed now with the caveat that to this point we have regulated only one positive CLE.

We recall that Oseledec showed [52] under some general conditions of smoothness of the vector field that the eigenvalues of the matrix

$$\mathbf{OSL}(J,\mathbf{y}(0),\mathbf{p}) = \left\{ [\mathbf{Df}^J(\mathbf{y}(0),\mathbf{p})]^T \cdot [\mathbf{Df}^J(\mathbf{y}(0),\mathbf{p})] \right\}^{1/2J} \tag{25}$$

as $J \to \infty$ (a) exist, (b) are independent of $\mathbf{y}(0)$ within a basin of attraction, and (c) are unchanged under a smooth coordinate transformation. A superscript T means the transpose of a matrix.

$\mathbf{Df}^J(\mathbf{y}(0),\mathbf{p})$ is defined, for example, in the solution to the equation for

$$\frac{\partial y_c(n)}{\partial y_a(0)} \tag{26}$$

via

$$\begin{aligned} \frac{\partial y_a(J+1)}{\partial y_b(0)} &= Df_{ac}(\mathbf{y}(J),\mathbf{p}) Df_{cd}(\mathbf{y}(J-1),\mathbf{p}),\ldots,Df_{eb}(\mathbf{y}(1),\mathbf{p}) \\ &= Df^J(\mathbf{y}(0),\mathbf{p})_{ab}, \end{aligned} \tag{27}$$

noting that $\frac{\partial y_a(0)}{\partial y_b(0)} = \delta_{ab}$.

A note on terminology: The eigenvalues of the Oseledec matrix must lie within the unit circle for stability. We call these σ_a, $a = 1, 2, \ldots$. Their logarithms $\lambda_a = \log(\sigma_a)$ are the Lyapunov exponents. Lyapunov numbers within the unit circle correspond to negative Lyapunov exponents.

When we add a coupling $k(x_1(n) - y_1(n))$ to the dynamics of the vector field $\mathbf{f}(\mathbf{y},\mathbf{p})$, the Jacobian matrix at each step changes to $Df_{ab} \to Df_{ab} - \delta_{11}k$. The eigenvalues of $\mathbf{OSL}(J,\mathbf{y}(0),\mathbf{p})$ for this modified Jacobian as $J \to \infty$ must lie within the unit circle to ensure the stability of the synchronization manifold.

To determine whether the parameter and state estimation approach that we discuss below will accomplish its goals, one should examine the CLEs produced by the Oseledec algorithm for values of $k > k_s$ where one has an indication of synchronization from the computation of the cost function,

$$C(\mathbf{y},\mathbf{p},k) = \frac{1}{2N} \sum_{n=0}^{N-1} \left\{ (x_1(n) - y_1(n))^2 \right\}, \tag{28}$$

as a function of k. The largest positive CLE determined by $\mathbf{OSL}(J,\mathbf{y}(0),\mathbf{p})$ becomes negative where this cost function exhibits synchronization. Equivalently, the largest eigenvalue of $\mathbf{OSL}(J,\mathbf{y}(0),\mathbf{p})$ lies within the unit circle.

If this cost function does not exhibit synchronization, then we conclude that the model does not synchronize with itself when presented information solely about $x_1(n)$. In the same

Copyright © by SIAM. Unauthorized reproduction of this article is prohibited.

Downloaded 11/01/17 to 161.45.254.242. Redistribution subject to SIAM license or copyright; see http://www.siam.org/journals/ojsa.php

circumstances, the largest CLE does not become negative as k is varied. It is quite important to examine this to assure oneself that the regularization procedure, here adding $k(x_1(n)-y_1(n))$ to the equation for $y_1(n+1)$, can work. This is always a good "pretest" of a model before presenting it experimental data.

With a single scalar control we can expect to regularize a single CLE associated with stability of the synchronization manifold. When we encounter more than one positive CLE, we will require more information from the data stream $x_1(n)$ and richer controls. We address this in a later section.

3. Variable coupling of the data and model: An extended Luenberger observer. To address the problems with a constant coupling of data into the model, we take two steps:

- First, we recognize that the solutions of typical nonlinear problems are not homogeneous in state space either on the attractor or in their motion though the space, so a control to the synchronization manifold could vary along a time series (and thus as the orbit moves through state space). This suggests replacing the constant k with a coupling that varies along orbits. We replace constant k, then, with $k \to u(t_n)$.
- Second, we want the strength of the coupling or "observer gain" to diminish to zero by the end of the estimation procedure. One way is to schedule a change in k or $u(t)$ through an iterative process associated with the estimation. Another idea is to recognize that the couplings at each observation time point $u(t_n) = u(n)$ are parameters to be treated on an equal footing with the fixed parameters in the problem. This suggests introducing a penalty for $u(n) \neq 0$ into the cost function. There are many choices for a penalty function of the $u(n)$. They must go to zero as $u(n) \to 0$, and perhaps the simplest is to select $u(n)^2$. If one wishes a different behavior for large $u(n)$, many choices are available. For example, a penalty function $\tanh[u(n)^2]$ is bounded above by unity but behaves as $u(n)^2$ for small $u(n)$. We have selected $u(n)^2$.

The addition of a time dependence to the coupling k is known in the control literature as an *extended* Luenberger observer [40, 41, 42, 43]. Some researchers seek a state variable dependence of this, so $k \to u(\mathbf{y}(n), n)$ is possible, but we have not found this to be required in practice. We combine the extended LO with an augmented cost function or optimization principle penalizing $u(n) \neq 0$, calling this *dynamical parameter estimation* (DPE), and we formulate it as the task of minimizing the cost function

$$C(\mathbf{y}, \mathbf{p}, u) = \frac{1}{2N} \sum_{n=0}^{N-1} \Big\{ (x_1(n) - y_1(n))^2 + u(n)^2 \Big\}, \tag{29}$$

subject to the equations of motion

$$\begin{aligned} y_1(n+1) &= f_1(\mathbf{y}(n), \mathbf{p}) + u(n)(x_1(n) - y_1(n)), \\ \mathbf{y}_R(n+1) &= \mathbf{f}_R(\mathbf{y}(n), \mathbf{p}), \end{aligned} \tag{30}$$

imposed as equality constraints in an optimization over $\mathbf{p}$, $\mathbf{y}(n)$, and $u(n)$. It is sometimes convenient to impose some smoothness criteria on the $u(n)$.

This problem is essentially that of optimally tracking a target trajectory $x_1(t)$ using a set of controls [54]. The formulation in [54] is not the same as we develop here. His control is a

Copyright © by SIAM. Unauthorized reproduction of this article is prohibited.

Downloaded 11/01/17 to 161.45.254.242. Redistribution subject to SIAM license or copyright; see http://www.siam.org/journals/ojsa.php

term $u(t)$ added to the model equation $\frac{dy_1(t)}{dt} = F_1(\mathbf{y}(t), \mathbf{p})$, rather than $u(t) * (x_1(t) - y_1(t))$, as when Kirk's book was written there was no concern about stabilization of a synchronization manifold.

Although not identified as such, the observer of chaos constructed in [2] is an extended LO. There they assumed knowledge of the fixed parameters $\mathbf{p}$ as well as detailed knowledge of the correct model for the observations. They were interested solely in estimation of the unobserved states $\mathbf{y}_R(n)$. They did connect their observer of chaotic states with an extended Kalman filter [55], noting that in the case of nonlinear systems it was neither an optimal filter nor a state estimator. In DPE we have given an optimization criterion for use with the LO and broadened its task to the estimation of model parameters and control parameters at each timestep $u(n)$ as well as estimating the unobserved states. By its formulation it is an optimal estimator.

In dealing with observed data the ability to monitor the $u(n)$ can be quite important. Below we suggest a consistency test for models using $u(n)$ that provides a way to assess the importance of the control in establishing synchronization.

4. Implementing DPE. There are many approaches to solving the numerical optimization problem posed by DPE. We have adopted the direct method which treats the fixed parameters $\mathbf{p}$, the state variables $\mathbf{y}(n)$, $n = 0, 1, \ldots, N-1$, and the control variables $u(n)$, $n = 0, 1, \ldots, N-1$, on the same footing and imposes the equations of motion

$$\begin{aligned} y_1(n+1) &= f_1(\mathbf{y}(n), \mathbf{p}) + u(n)(x_1(n) - y_1(n)), \\ \mathbf{y}_R(n+1) &= \mathbf{f}_R(\mathbf{y}(n), \mathbf{p}) \end{aligned} \tag{31}$$

as equality constraints in the $N(D+1)+L$-dimensional space of the $(\mathbf{p}, \mathbf{y}(n), u(n))$ on which the cost function or objective function $C(\mathbf{y}, \mathbf{p}, u)$ depends. There are $D(N-1)$ equality constraints on this optimization, leaving $N+D+L$ independent quantities. L of these are the fixed parameters $\mathbf{p}$. D of these are the $\mathbf{y}(0)$, and N of these are the $u(n)$, $n = 0, \ldots, N-1$, and should be zero when the optimization is completed. In the direct method all $N(D+1)+L$ quantities are treated on an equal footing. The equality constraints determine how many are independent. The particular implementation of the direct method we have employed in our calculations is called SNOPT [56, 57, 58, 59, 60]. It is publicly available; we have worked with the authors to provide an interface adapted to DPE problems, and we have written a MATLAB code to perform the various analytical derivatives of the vector field

$$\begin{aligned} & f_1(\mathbf{y}(n), \mathbf{p}) + u(n)(x_1(n) - y_1(n)), \\ & \mathbf{f}_R(\mathbf{y}(n), \mathbf{p}). \end{aligned} \tag{32}$$

Derivatives of a cost function and constraints are not required for SNOPT, as it includes a numerical differentiation algorithm; however, providing them simplifies the numerical task asked of the optimization program solving the DPE problem.

The direct method is closely related to multiple shooting [61, 62], where the interval over which data is available is divided into many steps, as here; the equality constraints, the differential equations, are implemented over each interval; and continuity at the endpoints of each interval is enforced. The critical difference here is in the use of a cost function and in the

Copyright © by SIAM. Unauthorized reproduction of this article is prohibited.

use of controls in the differential equations designed to stabilize the synchronization manifold. There may be detailed differences in the available software, SNOPT, and that for multiple shooting in how the mathematical optimization is carried out, but we have no comments on these in this paper. From our viewpoint, once the cost function has been specified to regularize orbits on the synchronization manifold, the choice of numerical method to solve the regularized optimization problem may be chosen for its own qualities.

4.1. The inner workings of DPE: A Hodgkin–Huxley example. We implemented DPE using SNOPT on a fairly standard Hodgkin–Huxley neuron model having four state variables representing the voltage $V(t)$ across the cell membrane as well as voltage gating variables for Na^+ and K^+ ion channels: $m(t)$, $h(t)$, and $n(t)$. The model takes the form [63]

$$\begin{aligned}
\frac{dV(t)}{dt} &= \frac{1}{C}\Big[g_{Na}m(t)^3h(t)(E_{Na}-V(t)) + g_K n(t)^4(E_K - V(t)) \\
&\qquad + g_L(E_L - V(t)) + I_{app}(t)\Big], \\
\frac{dm(t)}{dt} &= \alpha_m(V(t))(1-m(t)) - \beta_m(V(t))m(t), \\
\frac{dh(t)}{dt} &= \alpha_h(V(t))(1-h(t)) - \beta_h(V(t))h(t), \\
\frac{dn(t)}{dt} &= \alpha_n(V(t))(1-n(t)) - \beta_n(V(t))n(t).
\end{aligned} \tag{33}$$

In these equations the g's are conductances, the E's are reversal potentials, $I_{app}(t)$ is an externally imposed current injected into the cell, and the $\alpha(V)$'s and the $\beta(V)$'s are kinetic coefficients with a variety of fixed parameters describing the opening and closing of the ion channels. Altogether there are 22 fixed parameters, four state variables, and one control variable to be determined. As with any parameter estimation method, it is important that all of the parameters be able to be uniquely determined, and that any additional algebraic constraints on the parameters be enforced during the estimation procedure.

Calling the variables $V(t) = y_1(t)$, $m(t) = y_2(t)$, $h(t) = y_3(t)$, and $n(t) = y_4(t)$, we write the dynamical equations as

$$\begin{aligned}
\frac{dy_1(t)}{dt} &= p_1\{p_2 y_2(t)^3 y_3(t)(p_3 - y_1(t)) + p_4 y_3^4(t)(p_5 - y_1(t)) + p_6(p_7 - y_1(t)) + I_{app}(t)\} \\
&\quad + u(t)(x_1(t) - y_1(t)), \\
\frac{dy_2(t)}{dt} &= \frac{p_8(p_9 - y_1(t))(1-y_2(t))}{e^{p_{10}(p_9 - y_1(t))} - 1} - p_{11}e^{-p_{12}y_1(t)}y_2(t), \\
\frac{dy_3(t)}{dt} &= p_{13}e^{-p_{14}y_1(t)}(1-y_3(t)) - \frac{p_{15}}{e^{p_{16}(p_{17}-y_1(t))}+1}y_3(t), \\
\frac{dy_4(t)}{dt} &= \frac{p_{18}(p_{19}-y_1(t))}{e^{p_{20}(p_{19}-y_1(t))}-1}(1-y_4(t)) - p_{21}e^{-p_{22}y_1(t)}y_4(t).
\end{aligned} \tag{34}$$

We chose the parameters from a standard set for Hodgkin–Huxley models and solved these equations using an injected current $I_{app}(t)$ and $u(t) = 0$ to produce

$$[V_{data}(t), m_{data}(t), h_{data}(t), n_{data}(t)] = [x_1(t), x_2(t), x_3(t), x_4(t)]. \tag{35}$$

Copyright © by SIAM. Unauthorized reproduction of this article is prohibited.

Downloaded 11/01/17 to 161.45.254.242. Redistribution subject to SIAM license or copyright; see http://www.siam.org/journals/ojsa.php

Downloaded 11/01/17 to 161.45.254.242. Redistribution subject to SIAM license or copyright; see http://www.siam.org/journals/ojsa.php

Then, using the same model with undetermined parameters $p_1, \ldots, p_{22}$ and the same injected current $I_{app}(t)$, we evaluated

$$[y_1(t), y_2(t), y_3(t), y_4(t)], \tag{36}$$

utilizing the "observed" $V_{data}(t) = x_1(t)$ at $N = 4000$ time points separated by $\tau = 0.025\,\text{ms}$ (40 kHz sampling rate) presented to the model (observer). This would be 100 ms of data in an experimental setting, and this is quite feasible.

We minimized the objective function

$$C(p, \mathbf{y}, u) = \frac{1}{2N} \sum_{n=0}^{N-1} \Big\{ (x_1(n) - y_1(n))^2 + u(n)^2 \Big\}, \tag{37}$$

subject to the equations of motion, and used this to estimate the fixed parameters and the unobserved gating variables. The optimization was in a 20,022-dimensional space with 15,996 equality constraints.

We allowed the fixed parameters and the state and control variables to vary over a wide range. If the parameters were positive, we chose the range to be $[0, \text{big}]$, with $\text{big} = 10^{20}$, and similarly, if the parameters were negative, we chose the range to be $[-\text{big}, 0]$. Gating variables were required to lie between 0 and 1, and voltages ranged between $[-\text{big}, \text{big}]$.

SNOPT works iteratively with an initial set $\{\mathbf{y}(n)_0, u(n)_0, \mathbf{p}_0\}$ selected by the user. It then produces a sequence

$$\begin{aligned} \{\mathbf{y}(n)_0, u(n)_0, \mathbf{p}_0\} &\to \{\mathbf{y}(n)_1, u(n)_1, \mathbf{p}_1\} \cdots \\ &\to \{\mathbf{y}(n)_{final}, u(n)_{final}, \mathbf{p}_{final}\}. \end{aligned} \tag{38}$$

We initialized the iterations with $\mathbf{y}(n)_0 = 0$ and $u(n)_0 = 0$. This choice did not appear to matter for the final result, though at times the number of iterations needed to reach an optimum solution was affected by this choice. We recorded the DPE/SNOPT estimate of the cost function, the state and control variables, and the fixed parameters at various intermediate iterations as well as after the final iteration when our accuracy criteria (by default a tolerance of 10^{-6} in SNOPT) were met.

In Figure 4(a) we display the known $V_{data}(n) = x_1(n)$ and the estimate $y_1(n)$ at an intermediate stage of the iterations. We see that SNOPT is already visibly successful in matching these. In panel (b) we show $u(n)$ at this intermediate iteration, and we see it is still quite substantial. In panel (c) we compare the output of DPE/SNOPT for the unobserved gating variables at this intermediate iteration and the known $[x_2(n), x_3(n), x_4(n)]$. At this stage that matching is not impressive.

In Figure 5(a) we display the known $V_{data}(n) = x_1(n)$ and the estimate $y_1(n)$ after the final iteration. We see that SNOPT is visibly successful in matching these. In panel (b) we show $u(n)$ after this final iteration, and we see that it is now essentially zero; it is of magnitude 10^{-13} with fluctuations of that size reflecting the roundoff accuracy in our calculations. In panel (c) we compare the output of DPE/SNOPT for the unobserved gating variables after the final iteration and the known $[x_2(n), x_3(n), x_4(n)]$. At this stage that matching is extremely accurate.

The estimated fixed parameters after the final iteration are shown in Table 1. They match the 22 known parameters used to generate the data within a few percent or better. We show these parameters in the table along with the estimation of the same parameters using precisely

Copyright © by SIAM. Unauthorized reproduction of this article is prohibited.

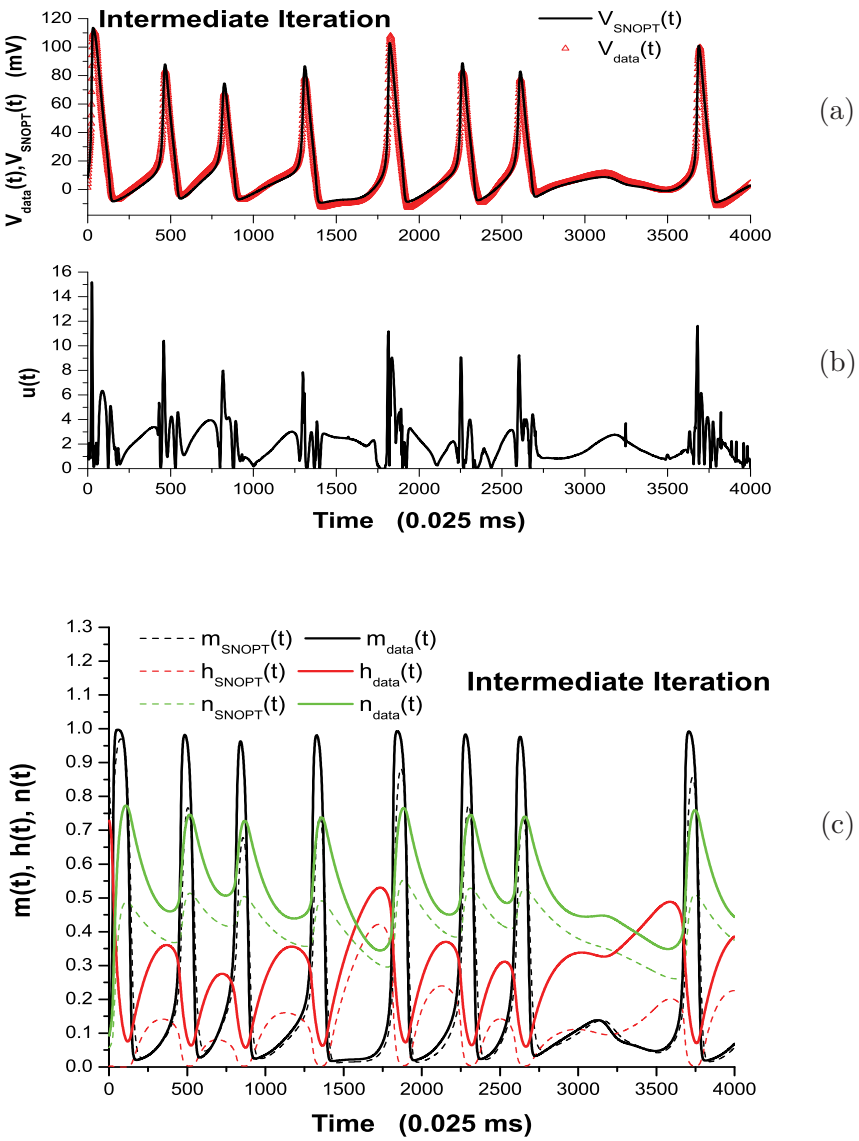

Figure 4. *Intermediate results in the DPE/SNOPT iterative estimation of the parameters and state variables for data from a Hodgkin–Huxley model.* (a) *DPE/SNOPT estimation of voltage in a Hodgkin–Huxley model.* (b) *Control, observer gain.* (c) *The unobserved gating variables in a Hodgkin–Huxley model.*

the same data for $x_1(n)$ and precisely the same algorithm, but setting all $u(n) = 0$ during the calculation. Since $u(n) = 0$ means we are using ordinary least squares, it is clear that it does not work well.

We found that by choosing the injected current $I_{app}(t)$ so that it drives the Hodgkin–Huxley model state well off the attractor familiar from the injection of DC currents, we were able to reach much more accurate estimates of the fixed parameters. In our example

Copyright © by SIAM. Unauthorized reproduction of this article is prohibited.

Downloaded 11/01/17 to 161.45.254.242. Redistribution subject to SIAM license or copyright; see http://www.siam.org/journals/ojsa.php

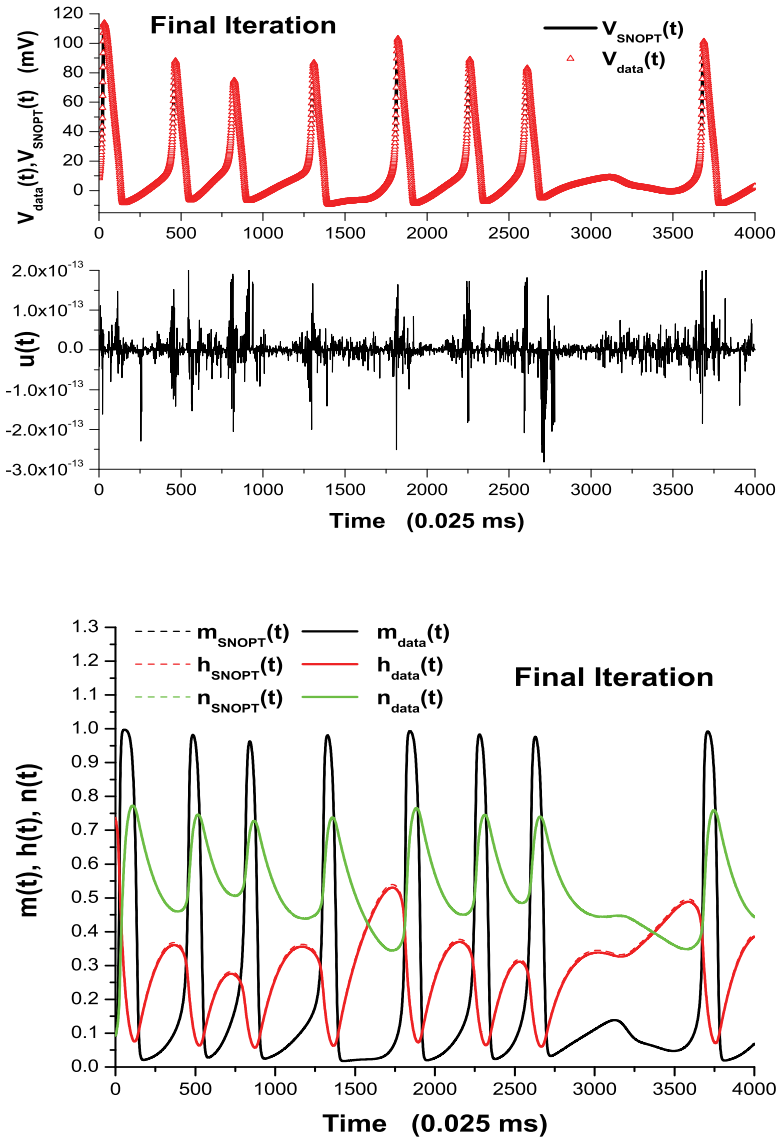

Figure 5. *Final results in the DPE/SNOPT iterative estimation of the parameters and state variables for data from a Hodgkin–Huxley model.* (a) *DPE/SNOPT estimation of voltage in a Hodgkin–Huxley model.* (b) *Control, observer gain.* (c) *The unobserved gating variables in a Hodgkin–Huxley model.*

we selected this current waveform from the output of the Lorenz model, but probably any waveform from a chaotic system should do. This takes advantage of the sensitivity of the orbits to small variations in the parameters, though, in principle, the parameters are independent of the applied current. We checked this last point by using a variety of different applied currents and found the same fixed parameters for this model.

The use of complex stimuli to explore the state space of neurons whose parameters we are

Downloaded 11/01/17 to 161.45.254.242. Redistribution subject to SIAM license or copyright; see http://www.siam.org/journals/ojsa.php

Copyright © by SIAM. Unauthorized reproduction of this article is prohibited.

Downloaded 11/01/17 to 161.45.254.242. Redistribution subject to SIAM license or copyright; see http://www.siam.org/journals/ojsa.php

Table 1

Estimation of the fixed parameters in a Hodgkin–Huxley model, (34), using DPE with SNOPT as the numerical optimization routine. In the rightmost column we present the results of the same estimation with DPE and SNOPT but holding all $u(n)$ fixed at zero during the computation. The latter procedure is the usual least squares estimation method using the direct method for numerical optimization and imposing the differential equations as equality constraints.

Parameter	Data	DPE	DPE $u = 0$
p_1	1.0	1.004	1.447
p_2	120.0	119.162	10.0
p_3	115.0	115.007	10.0
p_4	36.0	36.14	5.0
p_5	-12.0	-12.015	-1.0
p_6	0.3	0.296	0.075
p_7	-10.613	-10.53	-8.0
p_8	0.1	0.09994	0.186
p_9	25.0	24.933	8.76
p_{10}	0.1	0.1002	0.01
p_{11}	4.0	3.991	15.11
p_{12}	0.05555	0.055508	0.086
p_{13}	0.07	0.0698	0.025
p_{14}	0.05	0.0503	0.025
p_{15}	1.0	0.9984	5.55
p_{16}	30.0	30.05	5.025
p_{17}	0.1	0.09989	0.025
p_{18}	0.01	0.00996	0.0075
p_{19}	10.0	10.222	40.24
p_{20}	0.1	0.0989	0.064
p_{21}	0.125	0.12488	0.45
p_{22}	0.0125	0.012564	0.15

estimating may be especially valuable when the neuron has chaotic oscillations itself [64, 65].

4.2. Model consistency. We have no guarantee that the physically based model we construct, $\mathbf{y}(n+1) = \mathbf{f}(\mathbf{y}(n), \mathbf{p})$, is the correct representation of the data source; indeed, one can always expect model errors. We need to address the concern that if we achieve a small cost function, it might result because the control terms $u(n)(x_1(n) - y_1(n))$ are driving the model to the data on the synchronization manifold. The usual challenge for testing one's model is to subject it to new initial conditions $\mathbf{y}(0)$ or new driving forces, such as the external currents in the Hodgkin–Huxley model, and to compare those outcomes of the model with experiment.

We suggest also looking at a consistency test for model building that compares the size of the control term over the time series (or attractor) with the size of the model itself. In particular, we want the model term $f_1(\mathbf{y}(n), \mathbf{p})$ to be dominant over the additional control or regularization term when we have finished our parameter and state estimation through the numerical optimization. For this purpose, we suggest evaluating the following ratio $R(t)$ lying between 0, indicating an inconsistent model, and $R(t) \approx 1$, indicating a consistent model:

$$R^2(t_n) = \frac{[f_1(\mathbf{y}(t_n), \mathbf{p})]^2}{[f_1(\mathbf{y}(t_n), \mathbf{p})]^2 + [u(t_n)(x_1(t_n) - y_1(t_n))]^2}. \tag{39}$$

Copyright © by SIAM. Unauthorized reproduction of this article is prohibited.

Downloaded 11/01/17 to 161.45.254.242. Redistribution subject to SIAM license or copyright; see http://www.siam.org/journals/ojsa.php

If we evaluate $R(t)$ for our example of the Hodgkin–Huxley neuron model, we find $R(t) \approx 1$ across the time series used to estimate the unobserved states and parameters. In this example, of course, we knew the precise form of the system generating our "data," so the fact that our ratio is near unity for all time is a consistency check on the procedure rather than the model.

However, when we have observational data and do not know the underlying model for our data, we must use physical reasoning to develop the model, and then, having estimated the fixed parameters and the unobserved states, we can use this $R(t)$ criterion to establish the consistency of the model with the data. The power of knowing, from DPE, the unobserved states as well as the estimated values of the controls $u(n)$ becomes clear in the next section.

5. Using DPE with experimental data from a chaotic Colpitts oscillator. We built a circuit implementation of the Colpitts oscillator as shown in Figure 1 and measured $V_E(t)$, $V_C(t)$, and $I_L(t)$ for various values of the driving current I_0. The sampling time for the measurements was $\Delta t = 10\mu$s. Scaling the equations as in (20), we presented the dimensionless voltage $x_1(t) = \frac{V_E(t)}{V_T}$ to the model

$$\begin{aligned} \frac{dy_1(t)}{dt} &= p_1 y_2(t) + u(t)(x_1(t) - y_1(t)), \\ \frac{dy_2(t)}{dt} &= -p_3(y_1(t) + y_3(t)) - p_2 y_2(t), \\ \frac{dy_3(t)}{dt} &= p_4(y_2(t) + 1 - \exp(-(y_1(t) + p_5)). \end{aligned} \tag{40}$$

We now use DPE to estimate the parameters $p_1, \ldots, p_5$. We also wish to estimate the unobserved variables $V_C(t)$ and $I_L(t)$. To make this estimation we minimize

$$C(\mathbf{y}, u, \mathbf{p}) = \frac{1}{2N} \sum_{m=0}^{N-1} \Big\{ (x_1(m) - y_1(m))^2 + u(m)^2 \Big\}, \tag{41}$$

subject to (40).

We presented the model with data $x_1(t_n)$ taken with $I_0 = 7.10$mA and performed the DPE minimization. The minimum of $C(\mathbf{y}, u, \mathbf{p})$ starting from a variety of initial conditions was about 0.06, or an RMS (root mean square) variation from synchronization of about 0.25, with $p_1 = 2.862$, $p_2 = 0.0275$, $p_3 = 0.0091$, $p_4 = 0.1416$, and $p_5 = 25.24$. The value for p_5 corresponds to a current $I_s \approx 7.76 \times 10^{-14}$A, which is consistent with the characteristics of the transistor used in our experiments. The RMS variation of $y_1(m)$ was about 10.0, so this is a very small cost function relative to the natural variation of the data.

In Figure 6 we show the comparison of the estimated model output $y_1(t)$ with the scaled experimental signal $x_1(t) = V_E(t)/V_T$.

This looks like a very good fit to the data, but it is actually deceptive. The DPE approach also results in the sequence of controls $u(t_m)$ required to minimize the cost function subject to the equations of motion, (40). If we ask how important the control term $u(t)(x_1(t) - y_1(t))$ is relative to the vector field $F_1(\mathbf{y}(t), \mathbf{p}) = p_1 y_2(t)$ using the dimensionless ratio

$$R^2(t) = \frac{F_1(\mathbf{y}(t), \mathbf{p})^2}{F_1(\mathbf{y}(t), \mathbf{p})^2 + [u(t)(x_1(t) - y_1(t))]^2}, \tag{42}$$

Copyright © by SIAM. Unauthorized reproduction of this article is prohibited.

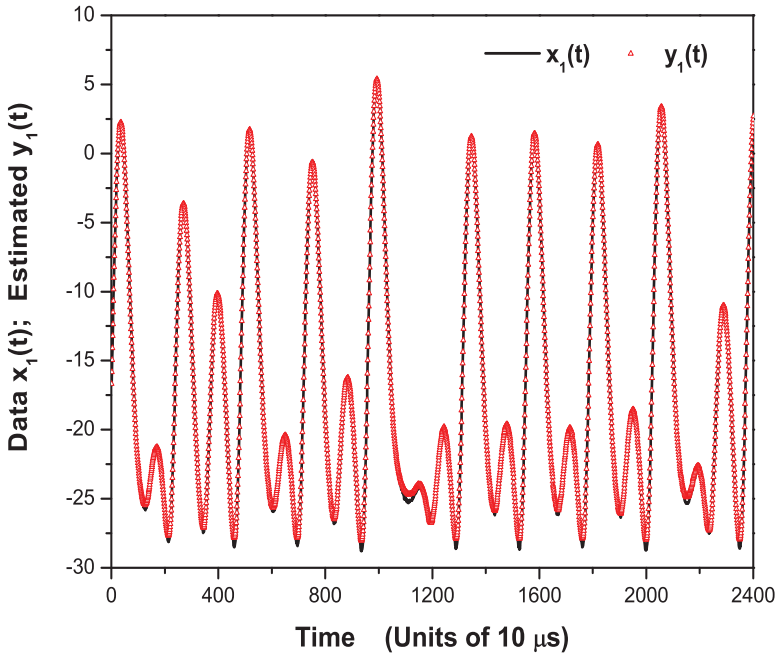

Figure 6. *Colpitts oscillator using data from the laboratory version of the circuit in Figure 1. A comparison of the dimensionless measured voltage* $x_1(t) = \frac{V_E(t)}{V_T}$ *with the estimation* $y_1(t)$ *using DPE and the model equation* (40).

as discussed above, we see in Figure 7 that this ratio deviates extensively from unity. $R(t) \approx 1$ would indicate a model consistent with the observed data, and we do not have that here. We can conclude that the model we have suggested for the Colpitts oscillator is not consistent with the data. The evaluation of the ratio $R(t)$ uses three estimated quantities: the fixed parameter p_1, the estimation of the unobserved (dimensionless and scaled) current through the inductor $y_2(t)$, and the estimated dimensionless form of $V_E(t)$: $y_1(t)$. This is the kind of information available from DPE through the regularization of the synchronization manifold.

In this example, we also had observations of the other variables $V_C(t)$ and $I_L(t)$, and using our estimated state variables $y_2(t)$ and $y_3(t)$, we could see that the DPE procedure did not produce a good estimation of those state variables. In the general experimental setting, we will not have this kind of information, so the $R(t)$ consistency check is expected to be of value.

It is likely that the physics of the nonlinear current-voltage curve for the transistor requires modification [66]. We do not pursue here how to improve the model, as our focus is on the information revealed by the estimation procedure, not on the physical reasoning required to establish a good model.

6. Many unstable directions transverse to the synchronization manifold. The discussion until now has focused on a scalar control $u(n)$ with which we can expect to move one positive CLE to a negative value and regulate orbits near the synchronization manifold. In general we anticipate there will be more than one positive CLE in complex systems, and we now discuss a model where we have evidence for two positive CLEs. There is only one fixed parameter, and we choose to focus our attention on determining the unobserved state variables only.

Copyright © by SIAM. Unauthorized reproduction of this article is prohibited.

Downloaded 11/01/17 to 161.45.254.242. Redistribution subject to SIAM license or copyright; see http://www.siam.org/journals/ojsa.php

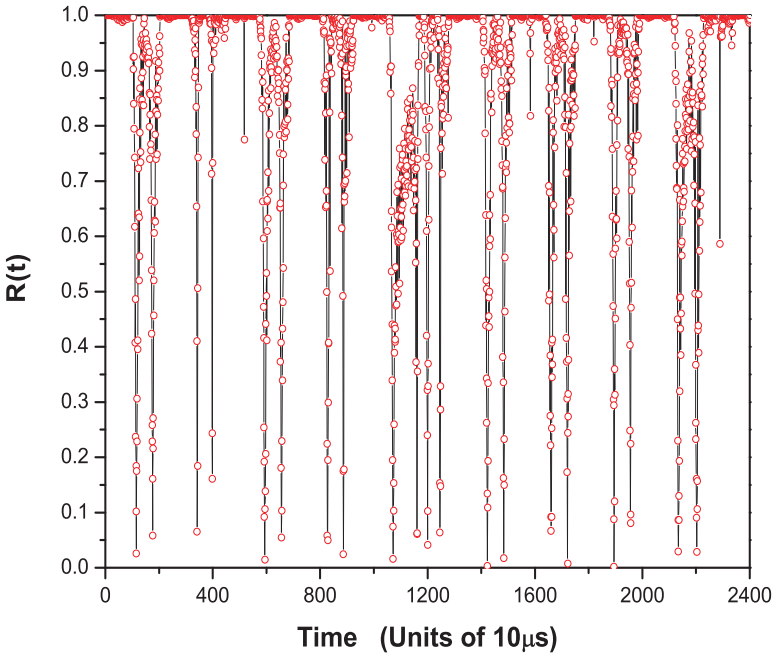

Figure 7. *The ratio equation (42) for the estimation of parameters and states using the observed dimensionless voltage* $\frac{V_E(t)}{V_T}$. *We see from this that the accuracy of the synchronization (Figure 6) matching the observed data for* $x_1(t) = \frac{V_E(t)}{V_T}$ *and the model voltage estimated using (40) is associated with the large magnitude of the controls* $u(t)$ *required along the synchronization manifold. These large deviations of the ratio* $R(t)$ *from* $R(t) = 1$ *indicate that the model is* not *consistent with the observed data.*

6.1. An example with two positive CLEs: The Lorenz 1996 model. In a discussion of predictability in atmosphere and ocean models, Lorenz [67] introduced a simple coupling of a "longitudinal variable" displayed on a circular lattice of length K. The model was meant to illustrate the westward flow of dynamical information, and it was used by Lorenz and Emanuel [68] to discuss strategies in selecting additional locations for dynamical weather variable measurements for the greatest improvement in analysis and forecasting. The model has one fixed parameter, the "forcing" f, and K dynamical variables, $x_a(t)$, $a = 1, 2, \ldots, K$, on a ring. The dynamical equations are

$$\frac{dx_a(t)}{dt} = x_{a-1}(t)(x_{a+1}(t) - x_{a-2}(t)) - x_a(t) + f, \qquad a = 1, 2, \ldots, K, \tag{43}$$

with $x_{-1}(t) = x_{K-1}(t)$, $x_0(t) = x_K(t)$, and $x_{K+1}(t) = x_1(t)$. Our interest is in locating a regime of parameters where synchronization of the model with itself requires the use of two pieces observed information. We selected $K = 5$ (Lorenz and Emanuel used $K = 40$) in which

$$\begin{aligned}
\frac{dx_1(t)}{dt} &= x_5(t)(x_2(t) - x_4(t)) - x_1(t) + f,\\
\frac{dx_2(t)}{dt} &= x_1(t)(x_3(t) - x_5(t)) - x_2(t) + f,\\
\frac{dx_3(t)}{dt} &= x_2(t)(x_4(t) - x_1(t)) - x_3(t) + f,
\end{aligned}$$

Downloaded 11/01/17 to 161.45.254.242. Redistribution subject to SIAM license or copyright; see http://www.siam.org/journals/ojsa.php

Copyright © by SIAM. Unauthorized reproduction of this article is prohibited.

$$\begin{aligned}\frac{dx_4(t)}{dt} &= x_3(t)(x_5(t) - x_2(t)) - x_4(t) + f,\\ \frac{dx_5(t)}{dt} &= x_4(t)(x_1(t) - x_3(t)) - x_5(t) + f.\end{aligned} \tag{44}$$

For f smaller than $f \approx 7.9$ the solutions exhibit a fixed point at $x_a(t) = f$ or limit cycles of various periods. For f somewhat greater than 8.0 chaotic behavior is seen. We selected $f = 8.17$ as a case to analyze; the orbits are chaotic for this value.

We generated data for $x_a(t)$ satisfying these differential equations using a timestep of $\Delta t = 0.01$, which corresponds to about $\frac{6}{5}\,h$ in the scales defined by the original model. Using the usual nonlinear time series analysis [35, 36] for one of the signals from this data set, we determined that the Lyapunov dimension associated with these exponents is $D_L = 4.6$.

We then asked whether we could synchronize the model for $y_a(t)$ with the same forcing parameter as in the data generating system using information on $x_1(t)$ alone. For this we made several calculations. The first coupled $x_1(t)$ to the equation for $y_1(t)$ as in the earlier sections of this paper. The model equations with driving by $x_1(t)$ read

$$\begin{aligned}\frac{dy_1(t)}{dt} &= y_5(t)(y_2(t) - y_4(t)) - y_1(t) + f + k_1(x_1(t) - y_1(t)),\\ \frac{dy_2(t)}{dt} &= y_1(t)(y_3(t) - y_5(t)) - y_2(t) + f,\\ \frac{dy_3(t)}{dt} &= y_2(t)(y_4(t) - y_1(t)) - y_3(t) + f,\\ \frac{dy_4(t)}{dt} &= y_3(t)(y_5(t) - y_2(t)) - y_4(t) + f,\\ \frac{dy_5(t)}{dt} &= y_4(t)(y_1(t) - y_3(t)) - y_5(t) + f.\end{aligned} \tag{45}$$

We found, as we will graphically show in a moment, that this did not result in synchronization when we evaluated

$$C(k_1) = \frac{1}{2N}\sum_{m=0}^{N-1}(x_1(t_m) - y_1(t_m))^2. \tag{46}$$

Following the suggestion in [2], we then coupled $x_1(t)$ to another dynamical variable using a different coupling k_2. We tried this for the $y_2(t)$ equation and also for the $y_3(t)$ equation with essentially similar results. We report on our experience with

$$\begin{aligned}\frac{dy_1(t)}{dt} &= y_5(t)(y_2(t) - y_4(t)) - y_1(t) + f + k_1(x_1(t) - y_1(t)),\\ \frac{dy_2(t)}{dt} &= y_1(t)(y_3(t) - y_5(t)) - y_2(t) + f,\\ \frac{dy_3(t)}{dt} &= y_2(t)(y_4(t) - y_1(t)) - y_3(t) + f + k_2(x_1(t) - y_1(t)),\\ \frac{dy_4(t)}{dt} &= y_3(t)(y_5(t) - y_2(t)) - y_4(t) + f,\end{aligned}$$

Downloaded 11/01/17 to 161.45.254.242. Redistribution subject to SIAM license or copyright; see http://www.siam.org/journals/ojsa.php

Copyright © by SIAM. Unauthorized reproduction of this article is prohibited.

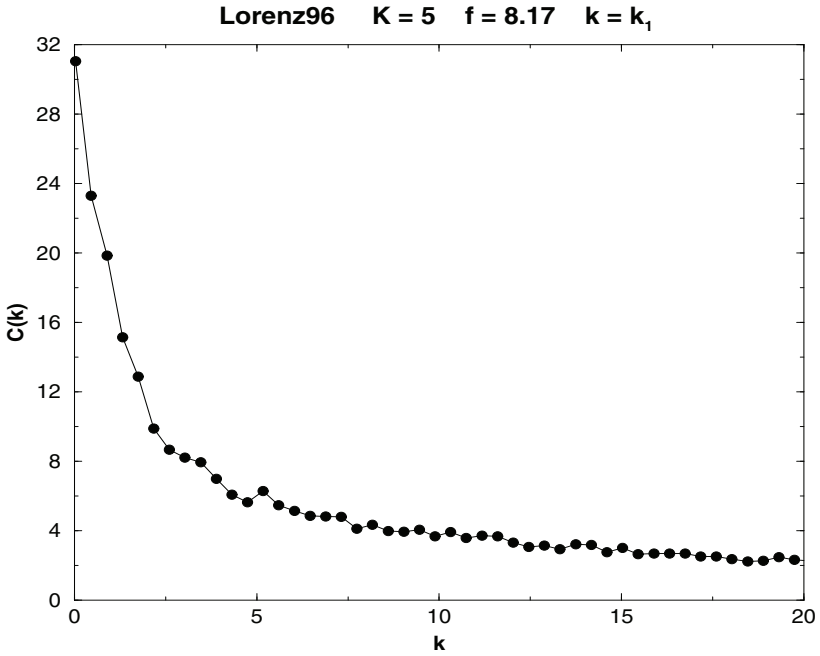

Figure 8. *Synchronization error as a function of k with $k_1 = k_2 = k$ associated with coupling information from $x_1(t)$ to the equations for $y_1(t)$ and $y_3(t)$ as in (47). This coupling scheme does not synchronize the two Lorenz96 systems, and it is an indication that more than one unstable direction is present on the synchronization manifold $\mathbf{x}(t) = \mathbf{y}(t)$.*

$$\frac{dy_5(t)}{dt} = y_4(t)(y_1(t) - y_3(t)) - y_5(t) + f. \tag{47}$$

In Figure 8 we show

$$C(k_1, k_2) = \frac{1}{2N} \sum_{m=0}^{N-1} (x_1(t_m) - y_1(t_m))^2, \tag{48}$$

for $k_1 = k_2$. In Figure 9 we display this as a function of both k_1 and k_2.

Finally, we coupled *both* $x_1(t)$ and $x_3(t)$ to the model equations for $y_a(t)$:

$$\begin{aligned}
\frac{dy_1(t)}{dt} &= y_5(t)(y_2(t) - y_4(t)) - y_1(t) + f + k_1(x_1(t) - y_1(t)),\\
\frac{dy_2(t)}{dt} &= y_1(t)(y_3(t) - y_5(t)) - y_2(t) + f,\\
\frac{dy_3(t)}{dt} &= y_2(t)(y_4(t) - y_1(t)) - y_3(t) + f + k_2(x_3(t) - y_3(t)),\\
\frac{dy_4(t)}{dt} &= y_3(t)(y_5(t) - y_2(t)) - y_4(t) + f,\\
\frac{dy_5(t)}{dt} &= y_4(t)(y_1(t) - y_3(t)) - y_5(t) + f,
\end{aligned} \tag{49}$$

Downloaded 11/01/17 to 161.45.254.242. Redistribution subject to SIAM license or copyright; see http://www.siam.org/journals/ojsa.php

Copyright © by SIAM. Unauthorized reproduction of this article is prohibited.

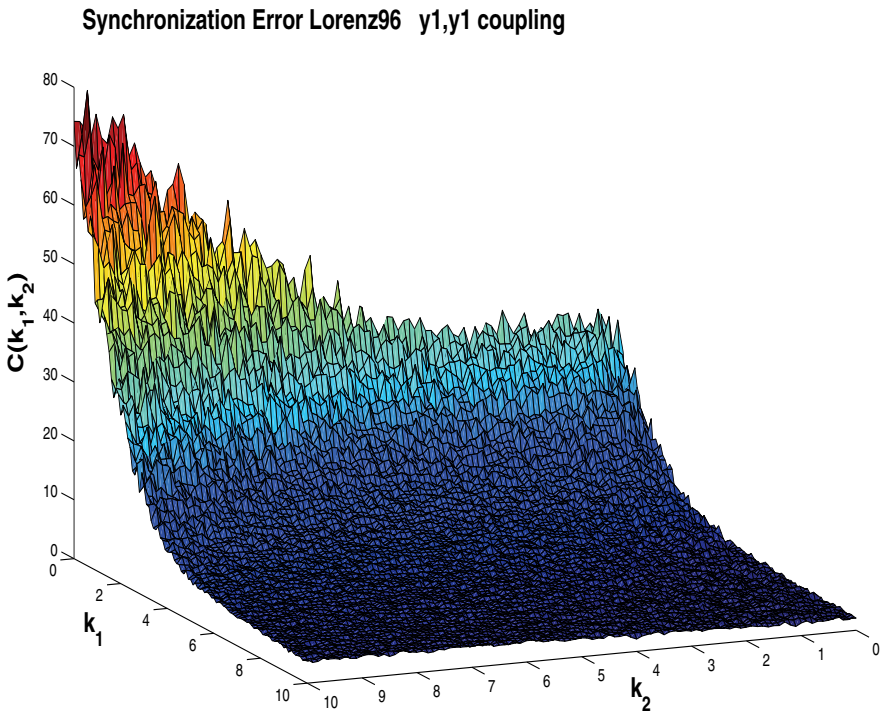

Figure 9. *Synchronization error as a function of k_1, k_2 associated with coupling information from $x_1(t)$ to the equations for $y_1(t)$ and $y_3(t)$ as in (47). This coupling scheme does not synchronize the two Lorenz96 systems, and it is an indication that more than one unstable direction is present on the synchronization manifold $\mathbf{x}(t) = \mathbf{y}(t)$.*

thus introducing new information beyond that carried by $x_1(t)$ alone into the coupling terms. In this case we find that for either $k_1 = 0$ or $k_2 = 0$ there is no synchronization of the data and the model. This is consistent with the previous result. However, when both k_1 and k_2 are effective, we see that the data and the model do synchronize.

In Figure 10 we show a cut through the k_1, k_2 dependence of the synchronization error $C_{x_1x_3}(k_1, k_2)$ arising from the coupling scheme (49) with $k_1 = k_2 = k$:

$$C_{x_1x_3}(k_1, k_2) = \frac{1}{2N} \sum_{m=0}^{N-1} \Big\{ (x_1(t_m) - y_1(t_m))^2 + (x_3(t_m) - y_3(t_m))^2 \Big\}. \tag{50}$$

The synchronization error has been reduced by a factor of 50 from the coupling scheme (47). In Figure 11 we display the three-dimensional version of this $C(k_1, k_2)$ as a function of both k_1 and k_2. This is a strong piece of evidence that two pieces of information on directions associated with the synchronization manifold $\mathbf{x}(t) = \mathbf{y}(t)$ are required to ensure synchronization.

The model now offers us the ability to ask whether we can, using DPE, present more information than a single measurement and accurately estimate $y_2(t)$, $y_4(t)$, and $y_5(t)$. The fact that the data and the model do not synchronize when only $x_1(t)$ is available indicates that we will not be able to estimate the unobserved variables if only $x_1(t)$ is presented to the

Copyright © by SIAM. Unauthorized reproduction of this article is prohibited.

Downloaded 11/01/17 to 161.45.254.242. Redistribution subject to SIAM license or copyright; see http://www.siam.org/journals/ojsa.php

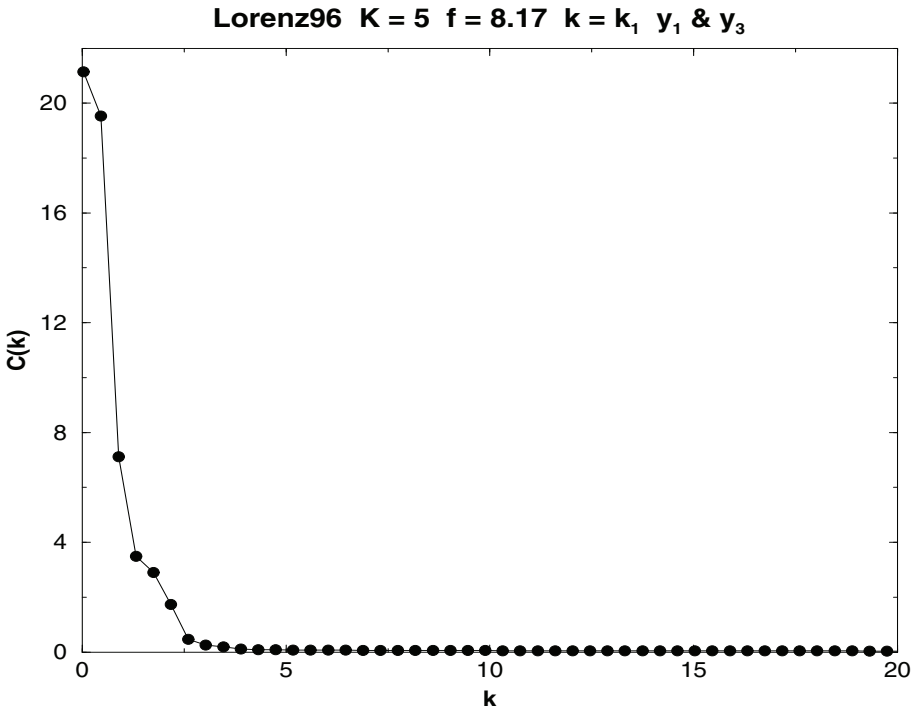

Figure 10. *Synchronization error as a function of k with $k_1 = k_2 = k$ associated with coupling information from $x_1(t)$ and $x_3(t)$ to the equations for $y_1(t)$ and $y_3(t)$ as in (49). The two systems now synchronize for k larger than about 3. This is an indication that two unstable directions are present on the synchronization manifold $\mathbf{x}(t) = \mathbf{y}(t)$.*

model. If we are able to take data for $x_1(t)$ and $x_3(t)$ over a time span t_0 to $t_0+T = t_0+N\Delta t$, and accurately estimate the unobserved variables at $t_0 + T$, then at time $t = t_0 + T$ we will have a complete picture of the state of the five-dimensional system (as we know the single parameter f here) and will be able to predict into the future $t > t_0+T$ within the usual limits on prediction of a chaotic system. We will have assimilated the data, $x_1(t)$ and $x_3(t)$, into our model and prepared ourselves for forecasting.

We now use the coupling scheme (49) with $k_1 \to u_1(t)$ and $k_2 \to u_2(t)$ to act as equality constraints on the minimization of the cost function

$$C(\mathbf{y},\mathbf{u}) = \frac{1}{2N}\sum_{m=0}^{N-1}\Big\{(x_1(t_m) - y_1(t_m))^2 + (x_3(t_m) - y_3(t_m))^2 + u_1(m)^2 + u_2(m)^2\Big\}. \tag{51}$$

We found that we could also estimate the parameter f quite accurately, but specifying it beforehand did not change any essential part of the calculations. The calculations we report now set $f = 8.17$.

We generated a data set from the Lorenz96 model with $K = 5$ and $f = 8.17$. As noted, this produced a chaotic time series on an attractor of dimension about 4.6. Using $N = 1635$

Copyright © by SIAM. Unauthorized reproduction of this article is prohibited.

Downloaded 11/01/17 to 161.45.254.242. Redistribution subject to SIAM license or copyright; see http://www.siam.org/journals/ojsa.php

Downloaded 11/01/17 to 161.45.254.242. Redistribution subject to SIAM license or copyright; see http://www.siam.org/journals/ojsa.php

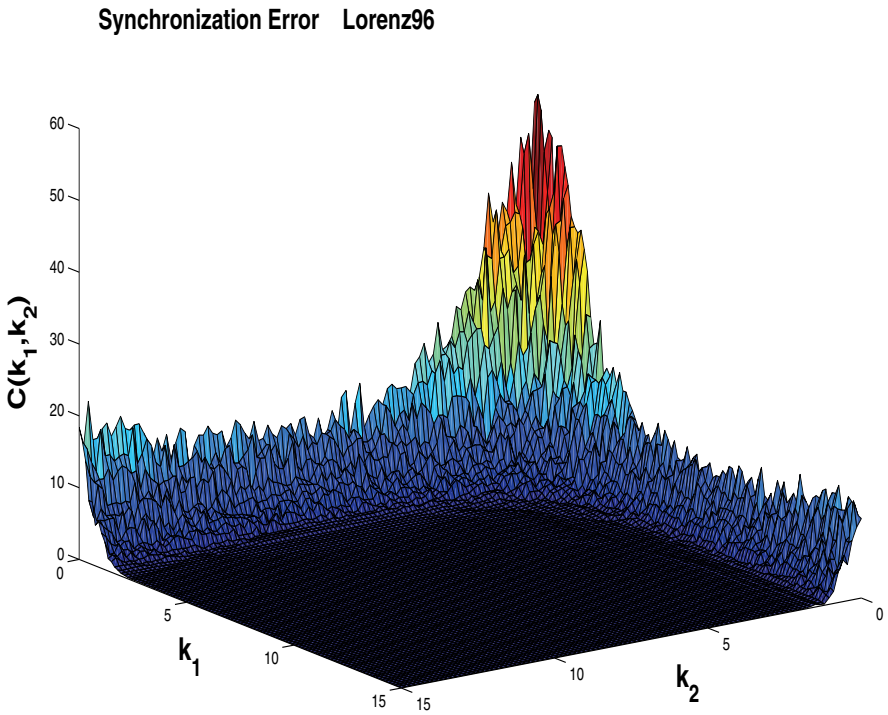

Figure 11. *Synchronization error as a function of k_1, k_2 associated with coupling information from $x_1(t)$ and $x_3(t)$ to the equations for $y_1(t)$ and $y_3(t)$ as in (49). The two systems now synchronize for k_1, k_2 each larger than about 3. This is an indication that two unstable directions are present on the synchronization manifold $\mathbf{x}(t) = \mathbf{y}(t)$.*

data points from $x_1(t)$ and $x_3(t)$, we used the dynamical parameter estimation algorithm to estimate the state variables in the model

$$
\begin{aligned}
\frac{dy_1(t)}{dt} &= y_5(t)(y_2(t) - y_4(t)) - y_1(t) + f + u_1(t)(x_1(t) - y_1(t)),\\
\frac{dy_2(t)}{dt} &= y_1(t)(y_3(t) - y_5(t)) - y_2(t) + f,\\
\frac{dy_3(t)}{dt} &= y_2(t)(y_4(t) - y_1(t)) - y_3(t) + f + u_2(t)(x_3(t) - y_3(t)),\\
\frac{dy_4(t)}{dt} &= y_3(t)(y_5(t) - y_2(t)) - y_4(t) + f,\\
\frac{dy_5(t)}{dt} &= y_4(t)(y_1(t) - y_3(t)) - y_5(t) + f. \qquad (52)
\end{aligned}
$$

In Figure 12 we see that over this segment of the data the variables $x_1(t)$ and $x_2(t)$ are well estimated. Similarly in Figure 13 we see that the variables $x_4(t)$ and $x_5(t)$ are well estimated. It was possible to achieve both a much smaller cost function and a better estimation by reducing the time step or the number of samples, but we selected this value of N since the chaotic motion of the orbits had already appeared. One can see this in a projection of two of

Copyright © by SIAM. Unauthorized reproduction of this article is prohibited.

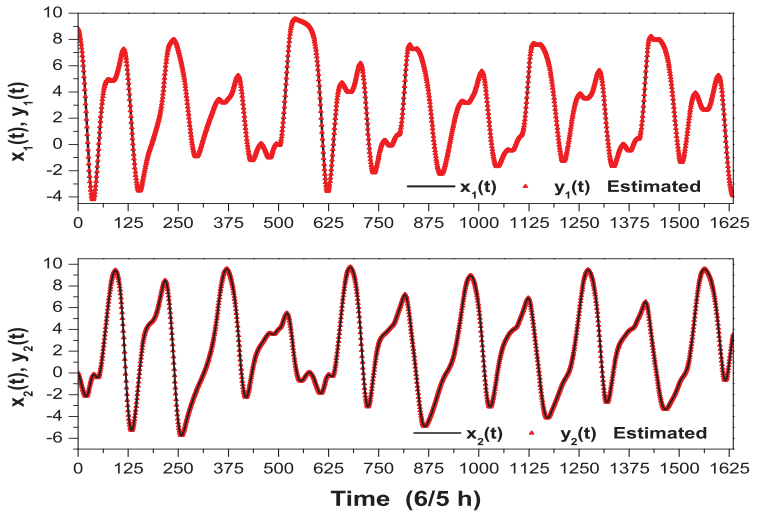

Figure 12. *Lorenz96 [67] model. The data $x_1(t), x_2(t)$ and the estimated model state variables $y_1(t), y_2(t)$.*

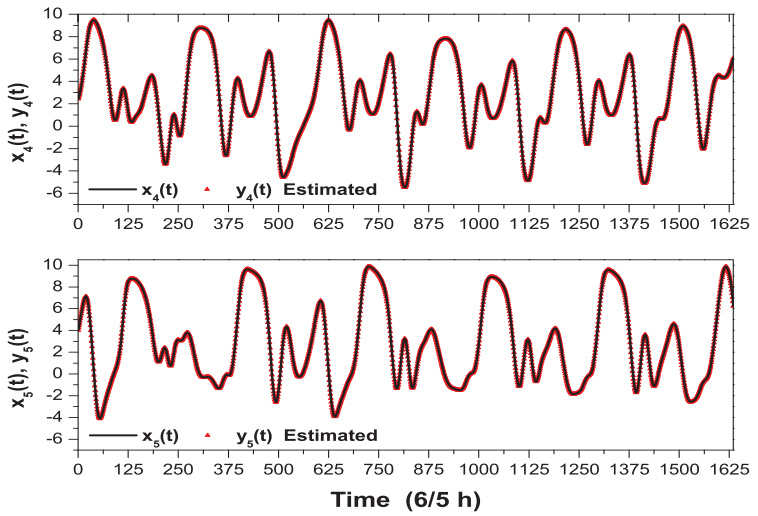

Figure 13. *Lorenz96 [67] model. The data $x_4(t), x_5(t)$ and the estimated model state variables $y_4(t), y_5(t)$.*

the dynamical variables, but we do not show this figure.

Now we took the values of the estimated state variables $y_a(t_N)$, $a = 1, 2, 3, 4, 5$, and the known value of $f = 8.17$, and we solved the five Lorenz96 differential equations for $t > t_N$ with $\mathbf{y}(t_N)$ as initial values. In Figure 14 we compared the predicted values $y_1(t > t_N)$ of the first component of the Lorenz96 model with the values $x_1(t > t_N)$; we also compared the predicted values $y_2(t > t_N)$ of the second component of the Lorenz96 model with the values $x_2(t > t_N)$. The predicted values remain close to the known values from the data set for about 1600 timesteps, or about 80 days of model time. Using the calculated Lyapunov exponents we would estimate that one should be able to predict about $\frac{1}{\lambda_1 \Delta t} \approx 1600$ timesteps for this model, depending on the accuracy of the given initial condition and the accuracy of the numerical calculation. In Figure 15 we show the same comparison between the known data and the

Copyright © by SIAM. Unauthorized reproduction of this article is prohibited.

Downloaded 11/01/17 to 161.45.254.242. Redistribution subject to SIAM license or copyright; see http://www.siam.org/journals/ojsa.php

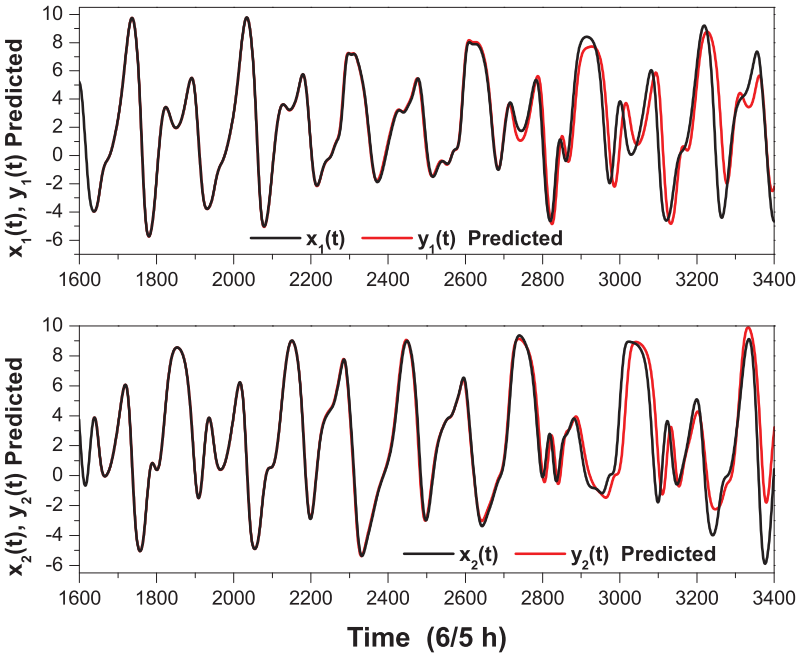

Figure 14. *Lorenz96 [67] model. The data for $x_1(t)$ and $x_2(t)$ along with the prediction for $t > 1635$ from the model for $y_1(t)$ and $y_2(t)$. The initial conditions of all state variables $y_a(t)$, $a = 1, 5$, at $t = 1635$ were estimated from 1635 points of $x_1(t)$ and $x_3(t)$ presented to the Lorenz96 ($K = 5$) model. The predictions are accurate for about 1500–1600 points beyond the new initial condition at $t = 1635$, and this is consistent with the estimation of the largest Lyapunov exponent as reported in the text.*

predictions for $y_4(t)$ and $y_5(t)$. Again the prediction is accurate about 1600 timesteps beyond the time point t_N where we began the calculation using the estimated state variables.

In Figure 16 we display the values of the two control variables $u_1(n), u_2(n)$ resulting from the SNOPT solution of the DPE optimization problem. Synchronization in this model occurs when these variables are of order 5, so one might suspect the validity of the calculation. However, examining the ratio tests

$$R_1(t) = \frac{F_1(\mathbf{y}(t), f)^2}{F_1(\mathbf{y}(t), f)^2 + [u_1(t)(x_1(t) - y_1(t))]^2},$$
$$R_3(t) = \frac{F_3(\mathbf{y}(t), f)^2}{F_3(\mathbf{y}(t), f)^2 + [u_2(t)(x_3(t) - y_3(t))]^2}, \tag{53}$$

where $F_a(\mathbf{y}, f)$ is the vector field for the dynamical variable $y_a(t)$ in (52), one finds $R_a(t) \approx 1.000$, and we conclude that the control terms are quite small with respect to the dynamical vector fields of the model. We also can state that this estimation of state variables and predictions of future behavior provide a consistent picture of the model system.

6.2. Time delay coordinates. In a large dynamical system, including interesting networks, one should expect more than one positive CLE. In that case we need more than the one-dimensional control of state space perturbations that we have with just a scalar $u(n)$. If we can observe many different (independent) variables in the experiment, then we would

Downloaded 11/01/17 to 161.45.254.242. Redistribution subject to SIAM license or copyright; see http://www.siam.org/journals/ojsa.php

Copyright © by SIAM. Unauthorized reproduction of this article is prohibited.

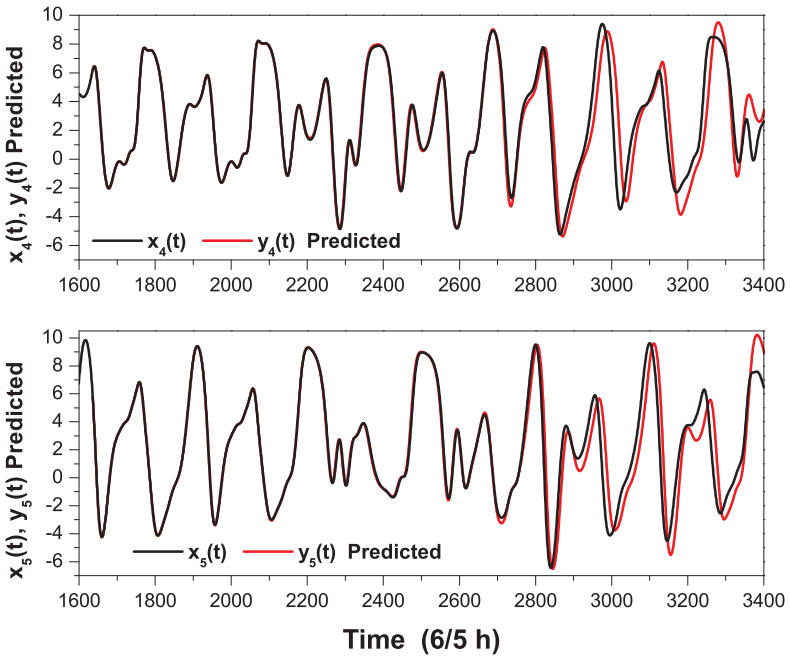

Figure 15. *Lorenz96 [67] model. The data for $x_4(t), x_5(t)$ and the predictions for $t > 1635$ from the model for $y_4(t), y_5(t)$. The initial conditions at $t = 1635$ were estimated from 1635 points of $x_1(t)$ and $x_3(t)$ presented to the Lorenz96 ($K = 5$) model. The predictions are accurate for about 1500–1600 points beyond the new initial condition at $t = 1635$, and this is consistent with the estimation of the largest Lyapunov exponent as reported in the text.*

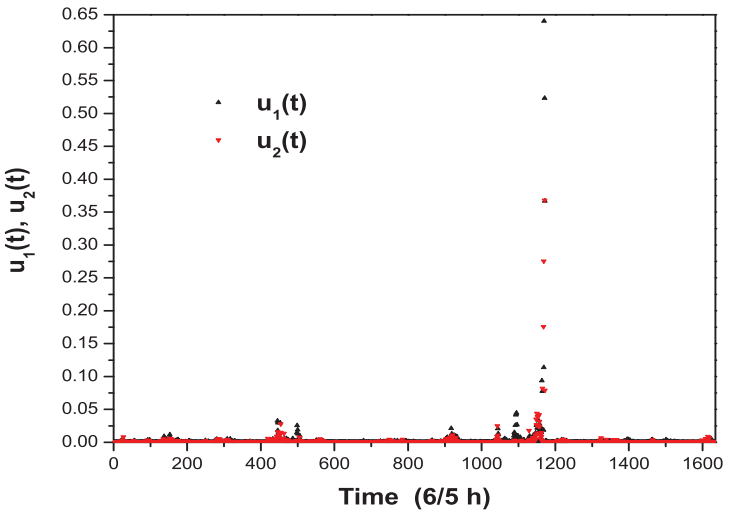

Figure 16. *Lorenz96 [67] model. The two controls $u_1(t)$ and $u_2(t)$ at the end of the estimation of the unobserved states for the Lorenz96, $K = 5$, model.*

have a chance to use them to move perturbed orbits back to the synchronization manifold. However, typically we do not have these additional observations. Our example of the Lorenz96

Copyright © by SIAM. Unauthorized reproduction of this article is prohibited.

Downloaded 11/01/17 to 161.45.254.242. Redistribution subject to SIAM license or copyright; see http://www.siam.org/journals/ojsa.php

Downloaded 11/01/17 to 161.45.254.242. Redistribution subject to SIAM license or copyright; see http://www.siam.org/journals/ojsa.php

system above took advantage of two measured observables, and, of course, if one has more than one independent observation, that is always useful. We proceed here assuming that we know only $x_1(n)$.

However, all is not lost. It is known both in nonlinear dynamics and in control theory that information is contained not only in the observations $x_1(t_n) = x_1(n)$ but also in the time delays of that observation [32, 33, 34], and there is, in the dynamics literature, an understanding of how many delays have new information about a given system [35, 36].

The new information in the measurement $x_1(n)$ not contained in $x_1(n-1)$ arises because in that one timestep of length τ, all the variables of the system are coupled to each other and particularly to x_1. They have operated over that timestep $t_n - t_{n-1}$ and influenced $x_1(n)$. Formally, this is just saying that $x_1(n) = f_1(x_1(n-1), \mathbf{x}_R(n-1), \mathbf{p})$ "knows" about the variables $\mathbf{x}_R(n-1)$, while $x_1(n-1)$ does not.

This suggests that we form the d-dimensional vector of time delay variables

$$[y_1(t_n), y_1(t_{n-1}), y_1(t_{n-2}), \ldots, y_1(t_{n-(d-1)})]. \tag{54}$$

In the dynamics literature this is known as time delay phase space reconstruction. It is a map from the space of physical variables $[y_1, \mathbf{y}_R]$ to an equivalent space time delay associated with a presumed diffeomorphism between the spaces [69]. How one determines the dimension d is interesting and well explored. It is known that a sufficient condition is $d = 2D + 1$.

The idea here is to cast the dynamics in the time delayed observer (model) space

$$\begin{aligned} \mathbf{s}(n) &= [y_1(n), y_1(n-1), \ldots, y_1(n-(d-1))] = [s_1(n), s_2(n), \ldots, s_d(n)], \\ s_\alpha(n) &= y_1(n-(\alpha-1)), \quad \alpha = 1, 2, \ldots, d. \end{aligned} \tag{55}$$

This is a map from $\mathbf{y} \to \mathbf{s}$: $\mathbf{s} = \phi(\mathbf{y})$.

In this space, the dynamics is

$$\begin{aligned} \mathbf{s}(n+1) &= [s_1(n+1), s_2(n+1), \ldots, s_d(n+1)] \\ &= [f_1(\mathbf{y}(n)), s_1(n), s_2(n), \ldots, s_{d-1}(n)], \end{aligned} \tag{56}$$

and using the inverse of the map $\mathbf{s} = \phi(\mathbf{y})$, namely $\mathbf{y} = \chi(\mathbf{s})$, we can write $f_1(\mathbf{y}(n), \mathbf{p}) = f_1(\chi(\mathbf{s}(n)), \mathbf{p}) = g(\mathbf{s}(n), \mathbf{p})$ to arrive at the time-delay space dynamics:

$$\mathbf{s}(n+1) = [g(\mathbf{s}(n), \mathbf{p}), s_1(n), s_2(n), \ldots, s_{d-1}(n)] = \mathbf{G}(\mathbf{s}(n), \mathbf{p}). \tag{57}$$

In this space we can introduce the coupling matrix $u_{\alpha\beta}(n)$, $\alpha, \beta = 1, 2, \ldots, d$, for the observer system

$$s_\alpha(n+1) = G_\alpha(\mathbf{s}(n), \mathbf{p}) + \sum_\beta u_{\alpha\beta}(n)(x_1(n-(\beta-1)) - s_\beta(n)). \tag{58}$$

We want the controls $u_{\alpha\beta}(n)$ to result in making all CLEs negative for the dynamics in time-delay space.

Copyright © by SIAM. Unauthorized reproduction of this article is prohibited.

Downloaded 11/01/17 to 161.45.254.242. Redistribution subject to SIAM license or copyright; see http://www.siam.org/journals/ojsa.php

The Oseledec multiplicative ergodic theorem comes into play here again. The role of the $u_{\alpha\beta}(n)$ is to change the effective Jacobian matrix

$$\frac{\partial G_\alpha(\mathbf{s}(n))}{\partial s_\beta(n)} \to \frac{\partial G_\alpha(\mathbf{s}(n))}{\partial s_\beta(n)} - u_{\alpha\beta}(n) \tag{59}$$

so that, iterated along an orbit of the dynamics $\mathbf{s}(n)$, it results in negative CLEs, thus stabilizing the synchronization manifold where $x_1(n-(\beta-1)) = s_\beta(n) = y_1(n-(\beta-1))$.

6.3. A two-dimensional example. We illustrate these ideas by working out the example of the dissipative "standard map" [37, 70, 71]. The map in "physical" coordinates is

$$\begin{aligned} y_1(n+1) &= y_1(n) + y_2(n) = f_1(y_1(n), y_2(n)), \\ y_2(n+1) &= Ay_2(n) - B\cos(y_1(n) + y_2(n)) = f_2(y_1(n), y_2(n)), \end{aligned} \tag{60}$$

with $0 \le A < 1$ and $B > 0$. The determinant of the Jacobian of this map is A. This map represents the angle, $y_1(n)$, and angular momentum, $y_2(n)$, of a pendulum with friction A, kicked with strength proportional to B at unit time intervals. If $A = 1$, this is a Hamiltonian system.

We suppose that data has been generated from this system and is presented to us as a measurement of the time series $x_1(n)$, $n = 0, 1, \ldots, N-1$. We wish to use our model in $\mathbf{y}(n) = [y_1(n), y_2(n)]$ to determine $A, B, y_2(0)$. For prediction from time $N-1$ forward we need both $y_1(N-1) = x_1(N-1)$ from the data and $y_2(N-1)$ as well as A and B from our estimation procedure.

We want to transform this to time-delay coordinates $[s_1(n) = y_1(n),\ s_2(n) = y_1(n-1)]$, and in this we are assuming that the dimension of the time-delay space is the same as that of the original space. In general, the embedding space (the time-delay space) may need to be of dimension 5.

The transformation from $[y_1, y_2]$ to $[s_1, s_2]$ is made using the inverse of the dynamics

$$\begin{aligned} y_1(n-1) &= y_1(n) - \frac{y_2(n) + B\cos(y_1(n))}{A}, \\ y_2(n-1) &= \frac{y_2(n) + B\cos(y_1(n))}{A}, \end{aligned} \tag{61}$$

and we have $\mathbf{s} = \phi(\mathbf{y})$:

$$\begin{aligned} s_1 &= \phi_1(y_1, y_2) = y_1, \\ s_2 &= \phi_2(y_1, y_2) = y_1 - \frac{y_2 + B\cos(y_1)}{A}. \end{aligned} \tag{62}$$

We can also determine the inverse of this, $\mathbf{y} = \chi(\mathbf{s})$:

$$\begin{aligned} y_1 &= \chi_1(s_1, s_2) = s_1, \\ y_2 &= \chi_2(s_1, s_2) = A(s_1 - s_2) - B\cos(s_1). \end{aligned} \tag{63}$$

Copyright © by SIAM. Unauthorized reproduction of this article is prohibited.

Downloaded 11/01/17 to 161.45.254.242. Redistribution subject to SIAM license or copyright; see http://www.siam.org/journals/ojsa.php

This allows us to transform the dynamics from $\mathbf{y}$-space to $\mathbf{s}$-space:

$$\begin{aligned} s_1(n+1) &= (1+A)s_1(n) - B\cos(s_1(n)) - As_2(n), \\ s_2(n+1) &= s_1(n), \end{aligned} \tag{64}$$

which we write as $s_\alpha(n+1) = G_\alpha(\mathbf{s}(n))$, $\alpha = 1, 2$.

Now we have incorporated all the information in the measured variable and its time delays into the dynamics in time-delay embedding space. If we had been required to use five dimensions to accomplish the embedding, we would have s_α, $\alpha = 1, 2, \ldots, 5$, coordinates and a more complicated mapping.

The idea is that now we have the ability to introduce controls into *all* of the coordinates in the dynamics. To this end we introduce the data vector

$$X(n) = [x_1(n), x_1(n-1)], \tag{65}$$

and introduce controls driving $s_\alpha(n)$ to the synchronization manifold $s_\alpha(n) = X_\alpha(n)$, into the time-delay dynamics

$$\mathbf{s}_\alpha(n+1) = G_\alpha(\mathbf{s}(n)) + U_\alpha(X(n), \mathbf{s}(n)), \tag{66}$$

where we require that the control $U_\alpha(X, \mathbf{s})$ vanish when we have synchronization $\mathbf{s}(n) = X(n)$; $\mathbf{U}(\mathbf{s}, \mathbf{s}) = 0$. In the linearized controls we used in earlier examples, $U_\alpha(X, \mathbf{s}) = \sum_\beta K_{\alpha\beta}(X_\beta - s_\beta)$.

We can now transform this from $\mathbf{s}$-space back to $\mathbf{y}$-space, knowing that we have introduced control to the synchronization manifold utilizing all the information carried by the data. In time-delay space we have

$$\begin{aligned} s_1(n+1) &= (1+A)s_1(n) - B\cos\big(s_1(n)\big) - As_2(n) + U_1\big(X(n), \mathbf{s}(n)\big), \\ s_2(n+1) &= s_1(n) + U_2\big(X(n), \mathbf{s}(n)\big), \end{aligned} \tag{67}$$

and this gives us

$$\begin{aligned} y_1(n+1) &= y_1(n) + y_2(n) + U_1(X(n), \phi(\mathbf{y}(n))), \\ y_2(n+1) &= Ay_2(n) - B\cos\big[y_1(n) + y_2(n) + U_1\big(X(n), \phi(\mathbf{y}(n))\big)\big] \\ &\quad + A\big[U_1\big(X(n), \phi(\mathbf{y}(n))\big) - U_2\big(X(n), \phi(\mathbf{y}(n))\big)\big]. \end{aligned} \tag{68}$$

If we are close to synchronization $X(n) \approx \mathbf{s}(n)$, and if we take the coupling $U_\alpha(X, \mathbf{s})$ to be linear $U_\alpha = \sum_\beta K_{\alpha\beta}(n)(X_\beta(n) - s_\beta(n))$, then we may write the physical space control in this approximation as

$$y_a(n+1) = f_a(y_1(n), y_2(n)) + \sum_b u_{ab}(n)(x_1(n-(b-1)) - y_1(n-(b-1))), \tag{69}$$

with

$$\begin{aligned} f_1(y_1, y_2) &= y_1 + y_2, \\ f_2(y_1, y_2) &= Ay_2 - B\cos(y_1 + y_2), \end{aligned} \tag{70}$$

Copyright © by SIAM. Unauthorized reproduction of this article is prohibited.

Downloaded 11/01/17 to 161.45.254.242. Redistribution subject to SIAM license or copyright; see http://www.siam.org/journals/ojsa.php

and

$$\begin{aligned} u_{1b}(n) &= K_{1b}(n), \\ u_{2b}(n) &= \big[A + B\sin(y_1(n) + y_2(n))\big]K_{1b}(n) - AK_{2b}(n). \end{aligned} \tag{71}$$

This suggests that, in a general format, the control to the synchronization manifold, that is the "gain" term in an extended LO, could be dependent on the phase space variables $\mathbf{y}(n)$. However, in our use of this formalism in practice, we have taken these controls or gains $u_{ab}(n)$ to be dependent on time alone.

6.4. General formulation. In a general formulation, we go from physical dynamics $\mathbf{y}(n+1) = \mathbf{f}(\mathbf{y}(n))$ to time-delay dynamics $\mathbf{s}(n+1) = \mathbf{G}(\mathbf{s}(n))$, and then we introduce the controls in the time-delay space $\mathbf{s}(n+1) = \mathbf{G}(\mathbf{s}(n)) + \mathbf{U}(X(n), \mathbf{s}(n))$. Next by applying the transformation $\mathbf{y} = \chi(\mathbf{s})$ to the $\mathbf{s}$-space dynamics with control, we have

$$\mathbf{y}(n+1) = \chi(\mathbf{s}(n+1)) = \chi[\mathbf{G}(\phi(\mathbf{y}(n))) + \mathbf{U}(X(n), \phi(\mathbf{y}(n)))]. \tag{72}$$

In general, we cannot explicitly display the transformations $\chi(\bullet)$ and $\phi(\bullet)$; however, if our control is succeeding in bringing the model to the data on their synchronization manifold, we can use the fact that $\mathbf{U}(X, \mathbf{s})$ is small to approximate the last expression via a Taylor expansion. In a linear approximation we may write $\mathbf{U}_\alpha(X, \mathbf{s}) \approx \sum_\beta K_{\alpha\beta}(X_\beta - s_\beta)$ and

$$\begin{aligned} \mathbf{y}_a(n+1) &\approx \chi_a(\mathbf{G}(s(n))) + \sum_{\alpha\beta} \frac{\partial \chi_a(\mathbf{G})}{\partial G_\alpha}\bigg|_{G_\alpha(s(n))} K_{\alpha\beta}(X_\beta(n) - s_\beta(n)) \\ &= f_a(\mathbf{y}(n)) + \sum_\beta u_{a\beta}(n)(X_\beta(n) - s_\beta(n)) \\ &= f_a(\mathbf{y}(n)) + \sum_\beta u_{a\beta}(n)(x_1(n-(\beta-1)) - y_1(n-(\beta-1))), \end{aligned}$$

where the controls are in a matrix $u_{a\beta}(n)$ coupling physical and time-delay embedding space. In general, they depend on the state space variables $\mathbf{y}$ through the dynamics.

To implement the requirement that when we have achieved synchronization of the data and the model the controls, introduced for regularization purposes, should vanish, we would add to the cost function a term proportional to $\mathbf{trace}[\mathbf{u}(\mathbf{y}(n))^T\mathbf{u}(\mathbf{y}(n))]$. This means our DPE procedure would read as follows:

Minimize

$$\begin{aligned} C(\mathbf{y}, \mathbf{u}, \mathbf{p}) = \frac{1}{2N}\sum_{n=0}^{N-1}\Bigg\{ &\sum_{\alpha=1}^{d}(x_1(n-(\alpha-1)) - y_1(n-(\alpha-1)))^2 \\ &+ \sum_{a=1}^{D}\sum_{\beta=1}^{d} u_{a\beta}(n)u_{a\beta}(n)\Bigg\}, \end{aligned} \tag{73}$$

subject to

$$\mathbf{y}_a(n+1) = f_a(\mathbf{y}(n)) + \sum_\beta u_{a\beta}(n)\Big[x_1(n-(\beta-1)) - y_1(n-(\beta-1))\Big]. \tag{74}$$

Copyright © by SIAM. Unauthorized reproduction of this article is prohibited.

We have written the control matrix $u_{a\beta}(n)$ as a function of time without indicating that it could also be a function of the state space variables $\mathbf{y}(n)$, allowing time to indicate where in state space the coupling is evaluated.

7. Conclusions and discussion. The goal of utilizing information in a data stream to complete a nonlinear dynamical model of the system producing that data stream has long been known to have two significant problems: (1) few of the many dynamical variables $\mathbf{x}(t)$ specifying the state of the observed system can, in fact, be observed, and (2) we wish to find parameters and initial conditions $\mathbf{y}(0)$ permitting the model dynamical variables $\mathbf{y}(t)$ to be close to the $\mathbf{x}(t)$. In other words, we seek synchronization of the data and the model, because in nonlinear systems chaotic behavior makes the state space manifold $\mathbf{y}(t) \approx \mathbf{x}(t)$ unstable.

The first challenge to using experimental observations means we must find a way to use those variables that can be observed to estimate those variables that are not observable. This has led to the idea of using the model, based on physical principles, as an "observer," allowing, through the model, the unobserved state variables to be estimated. The second challenge means that any metric (or cost function) of the closeness of the data $\mathbf{x}(t)$ and the model output $\mathbf{y}(t)$ must be stabilized. If one does not stabilize the motions near $\mathbf{x}(t) \approx \mathbf{y}(t)$, then a search for system fixed parameters or initial conditions will suffer from those instabilities and cause the search surface in parameter and initial condition space to be very irregular and possess numerous local minima, effectively hiding the desired good estimate.

In this paper we have analyzed the source of the irregularity in the parameter and initial condition surfaces of a closeness metric (we used standard least squares estimates of the synchronization of data $\mathbf{x}(t)$ and model output $\mathbf{y}(t)$) and showed how one can regulate this instability and allow a successful estimation search to proceed. Interestingly, as we regulated the parameter search, we found we had also stabilized the estimation of the unobserved state variables.

The combination of these goals was collected in a statement of dynamical parameter estimation (DPE). We investigated the foundation of the DPE algorithm both when there is one unstable direction associated with the synchronization manifold $\mathbf{x}(t) = \mathbf{y}(t)$ and when there are more than one unstable directions. In the first case we explored the implementation of our algorithm in the analysis of an electronic circuit, the Colpitts oscillator, and in the estimation of states and parameters in the Hodgkin–Huxley model of neural activity. We developed a formalism for the regularization of the synchronization manifold when there is more than one unstable direction associated with that manifold. We also explored a simple, geophysical model proposed by Lorenz [67] that expresses two unstable directions from the synchronization manifold, and showed how one can regularize that unstable configuration to allow for fixed parameter and unobserved state space estimation.

To the discussion of the ability of an observer or physically based model to estimate unobserved state variables, we added the Oseledec [52] multiplicative ergodic theorem. That theorem gives fundamental conditions indicating when the estimation of unobserved states will succeed.

Once one has identified the need to regularize instabilities on the synchronization manifold and identified an algorithm for achieving that along with estimating parameters and states in the physically based model one has developed, it is necessary to utilize some numerical optimization procedure to realize the success of the algorithm when dealing with nonlinear

Downloaded 11/01/17 to 161.45.254.242. Redistribution subject to SIAM license or copyright; see http://www.siam.org/journals/ojsa.php

Copyright © by SIAM. Unauthorized reproduction of this article is prohibited.

Downloaded 11/01/17 to 161.45.254.242. Redistribution subject to SIAM license or copyright; see http://www.siam.org/journals/ojsa.php

problems of interest. We used the "direct method" of numerical optimization, in which the states of a physically based model at discrete time points, observed data at those time points, controls to regularize the stability of the synchronization manifold, and fixed parameters in the nonlinear physical model are all treated on an equal footing. We implemented this method with the optimization software SNOPT [56, 57, 58, 59, 60], which is publicly available, well tested, and quite efficient. Of course there are many other numerical algorithms for addressing the DPE problem, and while we use SNOPT with some success, we are quite open to the use of other approaches to the numerical optimization challenge.

While one goal of the DPE approach is a method for estimating parameters, we showed in the Lorenz96 model that it can also accurately estimate state variables, allowing forecasts of the future development of a model from data assimilated over some earlier finite time segment. Further, this prediction or forecast was achieved for all state variables of the system, observed and unobserved. The Lorenz96 model that we used has five degrees of freedom, yet with the level of forcing we studied, it also has two positive CLEs. Our experience with that model suggests a clear, if numerically difficult, path to using the DPE methods for forecasts in much larger geophysical or neural network problems.

We have not explored the question of data from a dynamical system with multiple coexisting attractors—called multistability in the nonlinear dynamics literature. Through the direct method we search on parameters and state variables across the data window, and if we allow the initial values of the model variables to cover a large range, we expect that the correct basin of attraction will be reached because the time series within the data window should differ in important detail for each basin of attraction. It would, indeed, be interesting to see whether the numerical method we employ, or any numerical method, automatically selects the correct attractor when the range of values in the numerical search is large enough.

We also addressed the following issue. Suppose that one is presented with data from an experimental preparation, and, using the DPE method, a small cost function results in adjustment of the observed state variable, called $x_1(t)$ in this paper, so that it is close to the equivalent model variable, called $y_1(t)$, through the action of the control or coupling variable $u(t)$. Does this mean that the model for the variables $\mathbf{y}(t)$ proposed on physical grounds for the system producing the data $x_1(t)$ is a good model?

Validating, or more precisely invalidating [72], a model is a complex task. However, in the use of a coupling $u(t)$ to regulate the data/model synchronization manifold, we can as a matter of *consistency* ask whether the apparent synchrony among observable variables arises because of the role of the coupling or control $u(t)$ or is intrinsic to the model. By analyzing a dimensionless ratio of the model vector field size to the size of the coupling term, we presented and used a consistency test for the quality of a proposed model. We used this argument for consistency of our model for the Hodgkin–Huxley neuron parameter and state variable estimate as well as for our estimate of the initial conditions from which to make a predictive forecast for the Lorenz96 model. We also used it to argue for the inconsistency of the model we proposed for data taken from the nonlinear, chaotic Colpitts circuit. This set of outcomes of the consistency test suggests its usefulness for exploring and developing physical models for observed experimental data.

This paper has addressed three aspects of the state and parameter estimation problem in nonlinear systems:

Copyright © by SIAM. Unauthorized reproduction of this article is prohibited.

Downloaded 11/01/17 to 161.45.254.242. Redistribution subject to SIAM license or copyright; see http://www.siam.org/journals/ojsa.php

- Regulating the unstable behavior on the manifold where signals from a data source with state variables $\mathbf{x}(t)$ are asked to synchronize with a model of that source with state variables $\mathbf{y}(t)$. By reducing any positive conditional Lyapunov exponents (CLEs) [35, 48] to negative values locally on the synchronization manifold $\mathbf{x}(t) = \mathbf{y}(t)$, we produce a smooth search space on which to estimate both unknown fixed parameters in the model and unobserved state variables over the segment of time series from the source.
- Once the regulation has been achieved through the dynamical parameter estimation (DPE) algorithm, which asks that a cost function acting as a metric for synchronization $\mathbf{x}(t) \approx \mathbf{y}(t)$ plus a cost for the controls $\mathbf{u}(t)$ subject to the model equations with a coupling $\mathbf{u}(t)(\mathbf{x}(t) - \mathbf{y}(t))$ be minimized, then an appropriate numerical optimization algorithm needs to be implemented to acquire a solution to the optimization problem. We selected a method called SNOPT [56, 57, 58, 59, 60], which implements the direct method where the parameters, the model state variables, and the controls are treated on an equal footing. This is one of many numerical approaches to this optimization problem.
- When one is dealing, as is our goal, with observed data, not all components of the experimental system $\mathbf{x}(t)$ are observed. We also do not know a precise model for the system, but we are required to create a model from physical reasoning about the underlying dynamics. In this situation, we introduced a consistency check, measuring whether synchronization of the observed state variables with their model equivalents comes from the action of strong controls $\mathbf{u}(t)$ driving the model to synchronize with the data or from the consistent behavior of the model with no controls $\mathbf{u} = 0$.

These are three different aspects of the overall problem at hand, and each must be considered in establishing properties of a model for observation of data from a nonlinear system. The first item is the crux of the contribution in this paper, though the third item is also quite important.

Controls in the form of our $u_{\alpha\beta}(t)$ have been employed as constants for many years in the geophysical data assimilation literature, where they go by the name of nudging [73]. Typically these are constants added to equations of motion, whose role is to move the solutions to the dynamical equations toward the observations—that is, nudge the solutions. The size of the nudging terms is a matter of some discussion in this literature; while our results here indicate that the control terms can be quite large during the optimization process, at the end of the optimization they are driven to zero by the quadratic term in the cost function. Zero is an attractive value for the nudging terms, as they are typically not part of the physics of the problem at hand but are used to convey information from the data into the model. As our look into the optimization process for the Hodgkin–Huxley model calculation reported here demonstrates, the magnitude of the nudging during the optimization routine is not an issue, and the variation of the magnitudes of the controls over the attractor is to be expected.

The evaluation of the control terms to be zero at the end of the numerical optimization is consistent with their required nonzero values at early stages to overcome the synchronization manifold instability. This is reminiscent of other control problem where, when the control is effective, its value is small. It is only when synchronization is not being achieved, as at the start of our estimation calculations, that the control value needs to be large at some locations

Copyright © by SIAM. Unauthorized reproduction of this article is prohibited.

on the synchronization manifold.

While we have not addressed the issue of measurement noise in this paper, we have done so in our earlier paper applying some of these ideas in a neurobiological context [28]. We found that the estimation of both unobserved state variables and unknown parameters was accurate to within 5% when the signal-to-noise ratio for the "data" (called $x_1(t)$ here) was 20 dB or greater, but degenerated gracefully below that. We have not made a systematic study of the effects of noise in the measurements or, more difficult yet, noise in the environment affecting the model differential equations rather than the data.

Finally, it may be noted that the DPE algorithm for minimizing a cost function that includes costs for synchronization and for the controls, subject to model equations of motion with controls, is an optimal filter for nonlinear problems. Although, as is typically the case in nonlinear systems, no analytic solution is available, this constitutes an optimum filter in the sense of Kalman [55] for this problem.

Acknowledgments. Conversations with L. Pecora and D. Margoliash are gratefully acknowledged. We also appreciate E. Ott and F. Sorrentino sharing their unpublished manuscript with us. The anonymous referees of this paper enabled us to improve its clarity and address several important issues; many thanks for their diligence.

REFERENCES

[1] U. Parlitz and D. Yu, *Synchronization and Control Based Parameter Identification*, preprint, University of Goettingen, Göttingen, Germany, 2008.

[2] P. So, E. Ott, and W. P. Dayawansa, *Observing chaos: Deducing and tracking the state of a chaotic system from limited observation*, Phys. Rev. E, 49 (1994), pp. 2650–2660.

[3] H. D. I. Abarbanel, D. Creveling, and P. E. Gill, *State and parameter estimation in nonlinear systems as an optimal tracking problem*, Phys. Lett. A, 372 (2008), pp. 2640–2644.

[4] D. Creveling, J. Jeanne, and H. D. I. Abarbanel, *Parameter estimation using balanced synchronization*, Phys. Lett. A, 372 (2007), pp. 2043–2047.

[5] D. Creveling, J. Jeanne, and H. D. I. Abarbanel, *Estimation of parameters in nonlinear systems using balanced synchronization*, Phys. Rev. E, 77 (2008), paper 016208.

[6] U. S. Bhalla and J. M. Bower, *Exploring parameter space in detailed single neuron models: Simulations of the mitral and granule cells of the olfactory-bulb*, J. Neurophysiol., 69 (1993), pp. 1948–1965.

[7] M. C. Vanier and J. M. Bower, *A comparative survey of automated parameter-search methods for compartmental neural models*, J. Comput. Neurosci., 7 (1999), pp. 149–171.

[8] H. Dedieu and M. J. Ogorzalek, *Identifiability and identification of chaotic systems based on adaptive synchronization*, IEEE Trans. Circuits Systems I Fund. Theory Appl., 44 (1997), pp. 948–962.

[9] D. Haufler, F. Morin, J. C. Lacaille, and F. K. Skinner, *Parameter estimation in single-compartment neuron models using a synchronization-based method*, Neurocomput., 70 (2007), pp. 1605–1610.

[10] Q. J. Huys, M. B. Ahrens, and L. Paninski, *Efficient estimation of detailed single-neuron models*, J. Neurophysiol., 96 (2006), pp. 872–890.

[11] R. Konnur, *Synchronization-based approach for estimating all model parameters of chaotic systems*, Phys. Rev. E, 67 (2003), paper 027204.

[12] D. Huang, *Synchronization-based estimation of all parameters of chaotic systems from time series*, Phys. Rev. E, 69 (2004), paper 067201.

[13] A. Maybhate and R. E. Amritkar, *Use of synchronization and adaptive control in parameter estimation from a time series*, Phys. Rev. E, 59 (1999), pp. 284–293.

[14] H. Nijmeijer and I. M. Y. Mareels, *An observer looks at synchronization*, IEEE Trans. Circuits Systems I Fund. Theory Appl., 44 (1997), pp. 882–890.

Downloaded 11/01/17 to 161.45.254.242. Redistribution subject to SIAM license or copyright; see http://www.siam.org/journals/ojsa.php

Copyright © by SIAM. Unauthorized reproduction of this article is prohibited.

[15] U. Parlitz, *Estimating model parameters from time series by auto-synchronization*, Phys. Rev. Lett., 76 (1996), pp. 1232–1235.
[16] U. Parlitz, L. Junge, and L. Kocarev, *Synchronization based parameter estimation from time series*, Phys. Rev. E, 54 (1996), pp. 6253–6529.
[17] H. Sakaguchi, *Parameter evaluation from time sequences using chaos synchronization*, Phys. Rev. E, 65 (2002), paper 02720.
[18] I. Tokuda, U. Parlitz, L. Illing, M. B. Kennel, and H. D. I. Abarbanel, *Parameter estimation for neuron models*, in Proceedings of the 7th Experimental Chaos Conference, San Diego, CA, 2002.
[19] E. Tse, *Observer-estimators for discrete-time systems*, IEEE Trans. Automat. Control, AC-18 (1973), pp. 10–16.
[20] H. Voss, J. Timmer, and J. Kurths, *Nonlinear system identification from uncertain and indirect measurements*, Internat. J. Bifur. Chaos Appl. Sci. Engrg., 14 (2004), pp. 1905–1933.
[21] D. Yu, M. Righero, and L. Kocarev, *Estimating topology of networks*, Phys. Rev. Lett., 97 (2006), paper 188701.
[22] D. Dochain, *State and parameter estimation in chemical and biochemical processes: A tutorial*, J. Process Control, 13 (2003), pp. 801–818.
[23] G. Evensen, *Data Assimilation: The Ensemble Kalman Filter*, Springer, Berlin, Heidelberg, New York, 2007.
[24] Y. Sasaki, *Some basic formalisms in numerical variational analysis*, Monthly Weather Rev., 98 (1970), pp. 875–883.
[25] A. Tarantola, *Inverse Problem Theory and Methods for Model Parameter Estimation*, SIAM, Philadelphia, 2004.
[26] E. Kalnay, *Atmospheric Modeling, Data Assimilation and Predictability*, Cambridge University Press, Cambridge, UK, 2003.
[27] F. Sorrentino and E. Ott, *Using synchronization of chaos to identify the dynamics of unknown systems*, Chaos, 19 (2009), paper 033108.
[28] H. D. I. Abarbanel, P. Bryant, P. E. Gill, M. Kostuk, J. Rofe, Z. Singer, B. Toth, and E. L. Wang, *Dynamical parameter and state estimation in neuron models*, in Neuronal Variability and Its Functional Significance, M. Ding and D. Glanzman, eds., Oxford University Press, 2009, to appear.
[29] S. P. Garcia and J. S. Almeida, *Nearest neighbor embedding with different time delays*, Phys. Rev. E, 71 (2005), paper 037204.
[30] S. P. Garcia and J. S. Almeida, *Multivariate phase space reconstruction by nearest neighbor embedding with different time delays*, Phys. Rev. E, 72 (2005), paper 027205.
[31] Y. Hirata, H. Suzuki, and K. Aihara, *Reconstructing state spaces from multivariate data using variable time delays*, Phys. Rev. E, 74 (2006), paper 026202.
[32] F. Takens, *Detecting strange attractors in turbulence*, in Lecture Notes in Math. 898, Springer, Berlin, Heidelberg, 1981, pp. 366–381.
[33] D. Aeyels, *Generic observability of differentiable systems*, SIAM J. Control Optim., 19 (1981), pp. 595–603.
[34] D. Aeyels, *On the number of samples necessary to achieve observability*, Systems Control Lett., 1 (1981), pp. 92–94.
[35] H. D. I. Abarbanel, *The Analysis of Observed Chaotic Data*, Springer-Verlag, New York, 1996.
[36] H. Kantz and T. Schreiber, *Nonlinear Time Series Analysis*, 2nd ed., Cambridge University Press, Cambridge, UK, 2004.
[37] H. J. C. Huijberts, T. Lilge, and H. Nijmeijer, *Nonlinear discrete-time synchronization via extended observers*, Internat. J. Bifur. Chaos Appl. Sci. Engrg., 11 (2001), pp. 1997–2006.
[38] H. J. C. Huijberts, *On existence of extended observer forms for nonlinear discrete-time systems*, in New Directions in Nonlinear Observer Design, H. Nijmeijer and T. I. Fossen, eds., Springer, Berlin, 1999, pp. 77–92.
[39] T. Kailath, *Linear Systems*, Prentice–Hall, Englewood Cliffs, NJ, 1980.
[40] D. G. Luenberger, *Observing the state of a linear system*, IEEE Trans. Mil. Electron., 3MIL (1964), pp. 74–80.
[41] D. G. Luenberger, *Observers for multivariable systems*, IEEE Trans. Automat. Control, AC-11 (1966), pp. 190–197.

Downloaded 11/01/17 to 161.45.254.242. Redistribution subject to SIAM license or copyright; see http://www.siam.org/journals/ojsa.php

Copyright © by SIAM. Unauthorized reproduction of this article is prohibited.

[42] D. G. Luenberger, *An introduction to observers*, IEEE Trans. Automat. Control, AC-16 (1971), pp. 396–602.
[43] D. G. Luenberger, *Introduction to Dynamic Systems, Theory, Models and Applications*, Wiley, New York, 1979.
[44] G. Ciccarella, M. Dalla Morta, and A. Germani, *Observers for discrete time nonlinear systems*, Systems Control Lett., 20 (1993), pp. 373–382.
[45] G. Ciccarella, M. Dalla Morta, and A. Germani, *A robust observer for discrete time nonlinear systems*, Systems Control Lett., 24 (1995), pp. 291–300.
[46] P. E. Moral and J. W. Grizzle, *Observer design for nonlinear systems with discrete-time measurements*, IEEE Trans. Automat. Control, 40 (1995), pp. 395–404.
[47] B. Roset and H. Nijmeijer, *Observer-based model predictive control*, Internat. J. Control, 77 (2004), pp. 1452–1462.
[48] L. Pecora and T. Carroll, *Synchronization in chaotic systems*, Phys. Rev. Lett., 64 (1990), pp. 821–824.
[49] A. Pikovsky, M. Rosenblum, and J. Kurths, *Synchronization. A Universal Concept in Nonlinear Sciences*, Cambridge University Press, Cambridge, UK, 2001.
[50] K. Brueckner, *private communication*, UCSD, San Diego, CA, 1983.
[51] C. Pires, R. Vautard, and O. Talagrand, *On extending the limits of variational assimilation in nonlinear chaotic systems*, Tellus, 48A (1996), pp. 96–121.
[52] V. I. Oseledec, *A mutiplicative ergodic theorem, Lyapunov characteristic numbers for dynamical systems*, Trans. Moscow Math. Soc., 19 (1968), pp. 197–231.
[53] M. P. Kennedy, *Chaos in the Colpitts oscillator*, IEEE Trans. Circuits Systems I Fund. Theory Appl., 41 (1994), pp. 771–774.
[54] D. E. Kirk, *Optimal Control Theory: An Introduction*, Dover Publications, Mineola, NY, 1998 (originally published by Prentice–Hall in 1970).
[55] B. D. Anderson and J. B. Moore, *Optimal Filtering*, Dover Publications, Mineola, NY, 2005 (originally published by Prentice–Hall in 1979).
[56] A. Barclay, P. E. Gill, and J. B. Rosen, *SQP methods in optimal control*, in Variational Calculus, Optimal Control and Applications, Int. Ser. Numer. Math. 124, R. Bulirsch, L. Bittner, W. H. Schmidt, and K. Heier, eds., Birkhäuser, Basel, Boston, Berlin, 1998, pp. 207–222.
[57] P. E. Gill, W. Murray, and M. A. Saunders, *SNOPT: An SQP algorithm for large-scale constrained optimization*, SIAM J. Optim., 12 (2002), pp. 979–1006.
[58] P. E. Gill, W. Murray, and M. A. Saunders, *User's Guide for Snopt Version* 6*, A Fortran Package for Large-Scale Nonlinear Programming*, 2002; available online at http://www.cam.ucsd.edu/~peg/papers/sndoc6.pdf.
[59] P. Gill, W. Murray, and M. A. Saunders, *User's Guide for SNOPT* 5.3: *A Fortran Package for Large-Scale Nonlinear Programming*, technical report, Stanford Optimization Laboratory, Palo Alto, CA, 1997.
[60] P. E. Gill, W. Murray, and M. A. Saunders, *SNOPT: An SQP algorithm for large-scale constrained optimization*, SIAM Rev., 47 (2005), pp. 99–131.
[61] W. Horbelt, J. Timmer, and W. Melzer, *Estimating parameters in differential equations with application to physiological data*, in Differential Equations and Applications, G. Osipenko, ed., State Technical University, Saint Petersburg, Russia, 1998, pp. 23–33.
[62] W. Horbelt, *Maximum Likelihood Estimation in Dynamical Systems*, Ph.D. dissertation, Fakulät for Physik, Albert-Ludwigs-Universiät, Freiburg im Breisgau, Germany, 2001.
[63] C. Koch, *Biophysics of Computation: Information Processing in Single Neurons*, Oxford University Press, London, 2004.
[64] J. Guckenheimer and R. A. Oliva, *Chaos in the Hodgkin–Huxley model*, SIAM J. Appl. Dyn. Syst., 1 (2002), pp. 105–114.
[65] H. D. I. Abarbanel, R. Huerta, M. I. Rabinovich, N. F. Rulkov, P. F. Rowat, and A. I. Selverston, *Synchronized action of synaptically coupled chaotic model neurons*, Neural Comput., 8 (1996), pp. 1567–1602.
[66] J. C. Quinn, P. H. Bryant, D. R. Creveling, S. R. Klein, and H. D. I. Abarbanel, *Parameter and state estimation of experimental chaotic systems using synchronization*, Phys. Rev. E, 80 (2009), paper 016201.

Downloaded 11/01/17 to 161.45.254.242. Redistribution subject to SIAM license or copyright; see http://www.siam.org/journals/ojsa.php

Copyright © by SIAM. Unauthorized reproduction of this article is prohibited.

[67] E. N. Lorenz, *Predictability—A problem partly solved*, in Proceedings of the Seminar on Predictability, European Centre for Medium Range Weather Forecasting, Vol. 1, Reading, Berkshire, UK, 1996, pp. 1–18.
[68] E. N. Lorenz and K. A. Emanuel, *Optimal sites for supplementary weather observations: Simulation with a small model*, J. Atmospheric Sci., 55 (1998), pp. 399–414.
[69] T. Sauer, J. A. Yorke, and M. Casdagli, *Embedology*, J. Statist. Phys., 65 (1991), pp. 579–616.
[70] N. B. Tufillaro, T. Abbott, and J. Reilly, *An Experimental Approach to Nonlinear Dynamics and Chaos*, Addison–Wesley, Reading, MA, 1992.
[71] L. Cao, K. Judd, and A. Mees, *Targeting using global models built from nonstationary data*, Phys. Lett. A, 231 (1997), pp. 367–372.
[72] J. C. Doyle and R. S. Smith, *Model validation: A connection between robust control and identification*, IEEE Trans. Automat. Control, 31 (1992), pp. 942–952.
[73] P. J. Telford, P. Braesicke, O. Morgenstern, and J. A. Pyle, *Description and assessment of a nudged version of the new dynamics unified model*, Atmos. Chem. Phys., 8 (2008), pp. 1701–1712.

Downloaded 11/01/17 to 161.45.254.242. Redistribution subject to SIAM license or copyright; see http://www.siam.org/journals/ojsa.php

Copyright © by SIAM. Unauthorized reproduction of this article is prohibited.